Towards understanding biology of leydiogioma. G protein-coupled receptor and peroxisome proliferator-activated receptor crosstalk regulates lipid metabolism and steroidogenesis in Leydig cell tumors

Malgorzata Kotula-Balak[1§]*, Ewelina Gorowska-Wojtowicz[1§], Agnieszka Milon[1], Piotr Pawlicki[1], Alicja Kaminska[1], Laura Pardyak[1], Waclaw Tworzydlo[2], Bartosz J. Płachno[3], Anna Hejmej[1], Jan K. Wolski[4]

[1]Department of Endocrinology, Institute of Zoology and Biomedical Research, Jagiellonian University in Krakow, Poland, Gronostajowa 9, 30-387 Krakow, Poland; [2] Developmental Biology and Invertebrate Morphology, [3]Department of Plant Cytology and Embryology, Institute of Botany, Jagiellonian University in Kraków, Poland, Gronostajowa 9, 30-387 Krakow, Poland; [4]nOvum Fertility Clinic, Bociania 13, 02-807 Warszawa, Poland.

§ equal contribution

Correspondence to: *

e-mail: malgorzata.kotula-balak@uj.edu.pl

GPER-PPAR crosstalk and lipid metabolism in Leydig cell tumors

Abstract

Leydig cell tumors (LCT) are the most common type of testicular sex cord-stromal tumor. In this report, we implicate the G-coupled estrogen receptor (GPER) and peroxisome proliferator receptor (PPAR) in regulation of lipid homeostasis and the expression of steroidogenesis-controlling molecules in clinical specimens of LCTs and cell line (mouse tumor Leydig cells; MA-10). We also show the general structure and morphology of human LCTs with the use of scanning electron microscopy and light microscopy, respectively. In LCTs, protein immunoblotting and immunohistochemical analysis revealed increased expression of GPER and decreased expression of PPARα, β and γ. Concomitantly, changes in expression pattern of the lutropin receptor (LHR), protein kinase A (PKA), perilipin (PLIN), hormone sensitive lipase (HSL), steroidogenic acute regulatory protein (StAR), translocator protein (TSPO), HMG-CoA synthase (HMGCA), and HMG-CoA reductase (HMGCR) were observed.

Using MA-10 cells treated with GPER and PPAR antagonists (alone and in combination), we demonstrated there is a GPER-PPAR mediated control of cholesterol concentration. In addition, GPER-PPARα regulated estradiol secretion, while GPER-PPARγ affected cGMP concentration. It is assumed that GPER and PPAR can be altered in LCT, resulting in a perturbed lipid balance and steroidogenesis. In LCTs, the phosphatidylinositol-3-kinase (PI3K)-Akt-mTOR signaling pathway was disturbed. Thus, PI3K-Akt-mTOR, together with cGMP, can play a role in LCT proliferation, growth, and metastasis as well as lipid balance control.

In conclusion, we discuss the implications of GPER-PPAR interaction with lipid metabolism and steroidogenesis controlling-molecules in LCT biology that can be used in future studies as potential targets of diagnostic and therapeutic implementations.

Key words: G-coupled estrogen receptor; peroxisome proliferator-activated receptor; Leydig cell tumor; steroidogenesis-controlling molecules; ultrastructure

Introduction

Leydig cell tumor (LCT; leydigioma) is the most common non-germ cell gonadal tumor, accounting for 1-3% of all testicular tumors in adults and 4-9% in prepubertal children [1-3].

In recent years, a marked increase in the incidence of LCTs has been observed (14.7% of all testicular tumors removed). LCTs are usually benign tumors especially in infancy [4, 5], although local recurrence or metachronous tumors of the contralateral testis have also been described. Survival after diagnosis of primary LCTs ranged from 2 months to 17 years [6]. Patients with LCTs usually have symptoms of testicular swelling [7] or various endocrinological disruptions [8]. Some patients have associated issues with endocrine symptoms e.g. gynecomastia and decreased libido. Gynecomastia is the main clinical manifestation in adults, but it may also be clinically significant in affected children who undergo precocious puberty [9]. In the latter, behavioral perturbations were observed [10]. Some cases of LCTs were linked with increased plasma estradiol concentrations and were merely revealed by gynecomastia [11,12]. Moreover, infertility and azoospermia are not an unusual finding in patients with LCTs [13].

Less than 0.2% of all testicular cancers were evidenced by metastatic spread. Besides retroperitoneal nodes, other metastatic sites are liver, lungs, bone, and mediastinum [14, 15]. In prepubertal patients, even malignant LCTs are less likely to metastasize. Radical orchiectomy is the current standard of care but testis sparing surgery (TSS) (enucleation), in conjunction with intraoperative frozen section (FSE), has been recently attempted with promising results [16]. Prepubertal individuals and those with smaller tumors that lack evidence of malignancy are directly recommended for TSS.

The etiology of LCTs is unknown and appears heterogeneous. Furthermore, the molecular basis of LCTs is poorly understood. Some studies showed a possible role of genetic factors in LCT development. Interestingly, genetic mutations identified in children and adults were different and, in some cases, associated with other cancers [17]. In adults, it was observed that a somatic activating mutation in the guanine nucleotide-binding protein α gene may result in tumor development, leading to overexpression of the inhibin α subunit and hyperactivity of

sex steroid biosynthesis [5]. In addition, Carvajal-Carmona *et al.*, [18] reported an inherited fumarate hydratase mutation appears to cause tumor growth through activation of the hypoxia pathway. According to study of Lejeune *et al.*, [11] alterations in local stimuli, including Müllerian-inhibiting hormone, inhibin, growth factors, and temperature, may also create favorable conditions for initiation and development of LCTs.

Decreased Leydig cell function is common in men with reproductive disorders, including testicular dysgenesis syndrome (TDS). This syndrome is comprised of subfertility, cryptorchidism, hypospadias, and testicular cancer that is pathogenetically linked to impaired testis development and function [19, 20]. Leydig cell impairment manifests as a decreased testosterone/lutropin (LH) ratio and the presence of Leydig cell micronodules in the testis [21]. Additionally, uncontrolled synthesis and secretion of testosterone may suppress LH secretion and impair spermatogenesis [22]. The number and size of micronodules (clusters-when Leydig cell number >15) increases with the severity of TDS and increasing gonadotrophin levels [21, 23]. Due to ultrastructural changes demonstrated in Leydig cells within micronodules (decreased smooth endoplasmic reticulum, irregularly indented nuclear membrane, decreased lipofuscin pigment granules, and Reinke crystals) failure of their maturation is suggested [24, 25]. Also, the proportion of morphologically abnormal Leydig cells was inversely correlated with testosterone levels in patients with primary testicular disorders such as cryptorchidism, Klinefelter syndrome, and Del Castillo's syndrome [26]. Besides micronodules, other histopathological changes of Leydig cells have been described. In patients with germ cell tumors, Leydig cell hypertrophy and hyperplasia were linked to elevated levels of chorionic gonadotropin [27]. In addition, various chemicals induce Leydig cell hyperplasia because of disruption of the hypothalamic-pituitary-axis [28]. Neoplastic proliferation of Leydig cells may result in the synthesis of non-functional steroid hormones. Alternatively, an excess of various hormones (*e.g.* estrogen, prolactin) produce elevated LH

levels that excessively stimulate steroidogenic Leydig cell function [29]. Concomitantly, in experimental studies of animals exposed to hormones, hormonally active chemicals, or other hormonal modulators, Leydig cell hypertrophy was demonstrated [30-33]. However, there is no evidence as to whether Leydig cell pathology including micronodules, hyperplasia, and/or hypertrophy may further develop into leydigioma [34].

Mitogenicity associated with estrogen receptor-mediated cellular events is believed to be the mechanism by which estrogens contribute to tumorigenesis. Currently, implications of estrogen signaling *via* canonical estrogen receptors (ERs), G-protein coupled membrane estrogen receptor (GPER), as well as estrogen-related receptors (ERRs) is recognized in animal and human Leydig cell tumorigenesis [35-37]. Until recently, the function of GPER in testicular cells was only partially known. In human testis, Fietz *et al*. [38, 39] showed high levels of GPER mRNA expression in Leydig cells. In fact, not only is GPER able to bind sex steroids but also binds the peroxisome proliferator-activated receptors (PPARs) [40]. In amphibians, rodents, and humans, three forms of PPAR have been described to date: PPARα, PPARβ (also known as PPARδ), and PPARγ [41]. PPARs target genes that encode enzymes involved in peroxisome and mitochondria function as well as those of fatty acids, apolipoproteins, and lipoprotein lipase. Little is known about PPARs in the male reproductive system. In rat testis, PPARs are mainly expressed in Leydig and Sertoli cells [42]. It was shown that some PPAR chemicals alter testosterone production [43], and their long-term administration results in Leydig cell tumor development in rats [44, 45].

Scarce data are available on the molecular and biochemical characteristics of LCTs. Maintaining an adequate hormonal balance within the testis is the basis for proper gonadal function, thus playing a pivotal role for blocking hormone-secreting Leydig cell tumor development [46, 47]. Of note, in tumor cells, proliferation, growth, apoptosis, and communication are not only disturbed but other processes as well e.g. lipid metabolism [48].

148 It is worth noting that biosynthesis of sex steroids is multi-level, controlled process [49]. It
149 requires the coordinated expression of number of genes, proteins of various function
150 (receptors e.g. lutropin receptor; LHR, enzymes, transporters e.g. translocator protein; TSPO,
151 steroidogenic acute regulatory protein; StAR, and regulators), signaling molecules (e.g.
152 protein kinase A; PKA), and their regulators in response to LH stimulation. Moreover, for
153 cellular steroidogenic function, global lipid homeostasis is crucial. Perilipin (PLIN), hormone
154 sensitive lipase (HSL), and HMG-CoA synthase (HMGCS) and reductase (HMGCR) are
155 members of a cell structural and enzymatic protein machinery controlling lipid homeostasis
156 [50]. Activation of lipid metabolism is an early event in tumorigenesis, however, the precise
157 expression pattern of lipid balance-controlling molecules and their molecular mechanism
158 remains poorly characterized.
159 This study aims to determine the potential link between GPER and PPAR and whether
160 this interaction regulates lipid homeostasis in LCTs. To further investigate the relationship of
161 Leydig cell tumorigenesis to these receptors while elucidating the effects of their interactions
162 mouse tumor Leydig cells (MA-10) were utilized.

163 **Materials and Methods**

164 ***2.1. Tissue samples and ethical considerations***

165 Adult samples were residual tissues from testicular biopsy (microdissection TESE, by
166 Schlegel, 1998) specimens collected at the nOvum Fertility Clinic, Warsaw, Poland from
167 patients (31-45 year-old; n=24) diagnosed due to azoospermia (micronodules LCTs were
168 recognized during surgery) after written informed consent according to the approval
169 regulations by the National Commission of Bioethics at the Jagiellonian University in
170 Krakow, Poland; permit no. 1072.6120.218.2017 and were carried out in accordance with the
171 Declaration of Helsinki.

After evaluation by pathologists, the remaining tissue fragments were snap-frozen or fixed and paraffin-embedded, and stored at the Department of Endocrinology, Institute of Zoology and Biomedical Research, Jagiellonian University in Krakow, Poland.

2.2. Cell culture and treatments

The mouse Leydig cell line MA-10 was a generous gift from Dr. Mario Ascoli (University of Iowa, Iowa City, USA), and was maintained under standard technique [51]. Middle passages (p25-p28) of MA-10 cells were used for the study. The cells were grown in Waymouth's media (Gibco, Grand Island, NY) supplemented with 12% horse serum and 50 mg/l of gentamicin at 37 ^{o}C in 5% CO_2. Cells were plated overnight at a density of 1×10^5 cells/ml per well. Morphological and biochemical properties of MA-10 cells are regularly checked by microscopic observation, analysis of proliferation (TC20 Bio-Rad automated cell counter), mycoplasma detection (MycoFluor™ Mycoplasma Detection Kit; ThermoFisher Scientific), qRT-PCR analysis of characteristic genes and ELISA measurements of secretion products according to cell line authentication recommendations of the Global Bioresource Center (ATCC).

Twenty-four hours before the experiments, the medium was removed and replaced with a medium without phenol red supplemented with 5% dextran-coated, charcoal-treated FBS (5% DC-FBS) to exclude estrogenic effects caused by the medium. Next, cells were treated with selective antagonists: GPER [(3a*S**,4*R**,9b*R**)-4-(6-Bromo-1,3-benzodioxol-5-yl)-3a,4,5,9b-3*H*-cyclopenta[*c*]quinolone; G-15] (Tocris Bioscience, Bristol, UK), PPARα [*N*-((2*S*)-2-(((1*Z*)-1-Methyl-3-oxo-3-(4-(trifluoromethyl)phenyl)prop-1-enyl)amino)-3-(4-(2-(5-methyl-2-phenyl-1,3-oxazol-4-yl)ethoxy)phenyl)propyl) propanamide, GW6471] or PPARγ [2-Chloro-5-nitro-*N*-4-pyridinylbenzamide, T0070907] freshly prepared as 100nM stock solutions in dimethyl sulfoxide (DMSO) (Sigma-Aldrich) and stored at -20^{o}C. A stock concentrations

were subsequently dissolved in Waymouth's media to a final concentrations. Cells were treated with G-15, PPARα or PPARγ alone or together for 24hours. Doses of G-15 (10nM), PPARα (10μM) or PPARγ (10μM) [52]. Control cells were treated with DMSO (final conc. 0.1%). Cell lysates and culture media were frozen in -20^{o}C for further analyses.

2.3. Scanning electron microscopy analysis

LCTs were fixed in a mixture of 2.5% glutaraldehyde with 2.5% formaldehyde in a 0.05 M cacodylate buffer (Sigma; pH 7.2) for seven days, washed three times in a 0.1 M sodium cacodylate buffer and later dehydrated and subjected to critical-point drying. They were then sputter-coated with gold and examined at an accelerating voltage of 20 kV or 10 KV using a Hitachi S-4700 scanning electron microscope (Hitachi, Tokyo, Japan), which is housed in the Institute of Geological Sciences, Jagiellonian University in Kraków).

2.4. Histology

For routine histology, hematoxylin-eosin staining was performed on 4% paraformaldehyde LCT sections. As a control paraffin sections of human testis (cat. No. HP-401; Zyagen, San Diego, CA, USA) were used.

2.5. RNA isolation, reverse transcription and real-time quantitative RT-PCR

Total RNA was extracted from LCTs specimens and human Leydig cells (cat. no 10HU-103; ixCells Biotechnologies, San Diego CA, USA) using TRIzol® reagent (Life Technologies, Gaithersburg, MD, USA) according to the manufacturer's instructions. The yield and quality of the RNA were assessed using a NanoDrop ND2000 Spectrophotometer (Thermo Scientific, Wilmington, DE, USA). Samples with a 260/280 ratio of 1.95 or greater and a 260/230 ratio of 2.0 or greater were used for analysis. Total cDNA was prepared using High-Capacity cDNA

Reverse Transcription Kit (Applied Biosystems, Carlsbad, CA, USA) according to the manufacturer's instructions.

The purified total RNA was used to generate total cDNA. A volume equivalent to 1 µg of total RNA was reverse transcribed using the High-Capacity cDNA Reverse Transcription Kit (Applied Biosystems, Carlsbad, CA, USA) according to the manufacturer's instructions. Total cDNA was prepared in a 20-µL volume using a random primer, dNTP mix, RNase inhibitor and reverse transcriptase (RT). Parallel reactions for each RNA sample were run in the absence of RT to assess genomic DNA contamination. RNase-free water was added in place of the RT product.

Real-time RT-PCR was performed using the StepOne Real-Time PCR system (Applied Biosystems) and optimized standard conditions as described previously by Kotula-Balak et al. [53, 54]. Based on the gene sequences in Ensembl database primer sets were designed using Primer3 software (Table, supplementary material). Selected primers were synthesized by Institute of Biochemistry and Biophysics, Polish Academy of Science (Warsaw, Poland).

To calculate the amplification efficiency serial cDNA dilution curves were produced for all genes. A graph of threshold cycle (Ct) versus log10 relative copy number of the sample from a dilution series was produced. The slope of the curve was used to determine the amplification efficiency: $\%E = (10^{-1/slope}-1) \times 100$. All PCR assays displayed efficiency between 94% and 104%.

Detection of amplification gene products was performed with 10 ng cDNA, 0.5 µM primers, and SYBR Green master mix (Applied Biosystems) in a final volume of 20 µL. Amplifications were performed as follows: 55 °C for 2 min, 94 °C for 10 min, followed by annealing temperature for 30 s (Table 1) and 45 s 72 °C to determine the cycle threshold (Ct) for quantitative measurement. To confirm amplification specificity, the PCR products from each

246 primer pair were subjected to melting curve analysis and subsequent agarose gel electrophoresis
247 (not shown). In all real-time RT-PCR reactions, a negative control corresponding to RT reaction
248 without the reverse transcriptase enzyme and a blank sample were carried out. All PCR products
249 stained with Midori Green Stain (Nippon Genetics Europe GmbH, Düren, Germany) were run
250 on agarose gels. Images were captured using a Bio–Rad Gel Doc XR System (Bio–Rad
251 Laboratories, Hercules, CA, USA) (not shown). mRNA expressions were normalized to the *β-*
252 *actin* mRNA (relative quantification, RQ = 1) with the use of the $2^{-\Delta\Delta Ct}$ method.
253
254 ***2.6. Western blotting***
255 For quantification of protein expression (Table 1) from LCTs proteins (as a control human
256 Leydig cells; cat. No 10HU-103; ixCells Biotechnologies, San Diego CA, USA) were
257 extracted in 50 µl of radioimmunoprecipitation assay buffer (RIPA; Thermo Scientific, Inc.
258 Rockford IL, USA) and protease inhibitor cocktail (Sigma Chemical Co., St. Louis, Missouri,
259 USA). Concentration of proteins was determined with Bradford reagent (Bio-Rad Protein
260 Assay; Bio-Rad Laboratories GmbH, Munchen, Germany), using bovine serum albumin as a
261 standard. Aliquots (50 µg protein) of cell lysates were used for electrophoresis on 12% mini
262 gel by standard SDS-PAGE procedures and electrotransferred to polyvinylidene difluoride
263 (PVDF) membranes (Millipore Corporate, MA, USA) by a semi-dry transfer cell (Bio-Rad).
264 Then, blots were blocked with 5% nonfat dry milk in TBS, 0.1% Tween 20, overnight at 4 °C
265 with shaking, followed by an incubation with respective antibodies (Table 1). The membranes
266 were washed and incubated with a secondary antibody conjugated with the horseradish-
267 peroxidase labeled goat anti-mouse or goat anti-rabbit IgGs (Vector Labs., Burlingame, CA,
268 USA) at a dilution 1:1000, for 1 h at RT. Immunoreactive proteins were detected by
269 chemiluminescence with Western Blotting Luminol Reagent (Santa Cruz Biotechnology), and
270 images were captured with a ChemiDoc XRS + System (Bio-Rad Laboratories). All

immunoblots were stripped with stripping buffer containing 62.5 mM Tris–HCl, 100 mM 2-mercaptoethanol, and 2% SDS (pH 6.7) at 50 °C for 30 min and incubated in a rabbit polyclonal antibody against β-actin. Each data point was normalized against its corresponding β-actin data point.

To obtain quantitative results, immunoblots were scanned with Image Lab 2.0 (Bio-Rad Laboratories). Then, a bound antibody was revealed using DAB as the substrate. Finally, the membranes were dried and then scanned using Epson Perfection Photo Scanner (Epson Corporation, CA, USA). Molecular masses were estimated by reference to standard proteins (Prestained SDS-PAGE Standards, Bio-Rad Labs, GmbH, Munchen, Germany). Quantitative analysis was performed for three separately repeated experiments using a public domain ImageJ software (National Institutes of Health, Bethesda, MD) as described elsewhere [55]. The relative protein levels were expressed as arbitrary units.

2.7. Immunohistochemistry

To optimize immunohistochemical staining testis sections both control (Zyagen, San Diego, CA, USA) and LCTs sections were immersed in 10 mM citrate buffer (pH 6.0) and heated in a microwave oven (2 × 5 min, 700 W). Thereafter, sections were immersed sequentially in H_2O_2 (3 %; v/v) for 10 min and normal goat serum (5 %; v/v) for 30 min which were used as blocking solutions. After overnight incubation at 4 °C with primary antibodies listed in Table 1. Next respective biotinylated antibodies (anti-rabbit and anti-mouse IgGs; 1: 400; Vector, Burlingame CA, USA) and avidin-biotinylated horseradish peroxidase complex (ABC/HRP; 1:100; Dako, Glostrup, Denmark) were applied in succession. Bound antibody was visualized with 3,3'-diaminobenzidine (DAB) (0.05 %; v/v; Sigma-Aldrich) as a chromogenic substrate. Control sections included omission of primary antibody and substitution by irrelevant IgG.

296

297 ***2.8. Cholesterol assay***

298 The Amplex® Red Cholesterol Assay Kit (Molecular Probes Inc., Eugene, OR, USA) was
299 used for cholesterol content (μM) analysis in control and treated with GPER and PPAR (alone
300 or in combinations) MA-10 cells. For measurement 100 μl cell lysates was used according to
301 manufacturer' s protocol. Data were expressed as mean ± SD. The fluorescence (λ = 580 nm)
302 was measured with the use of a fluorescence multiwell plate reader SPARK Tecan,
303 Switzerland.

304 ***2.9. cGMP concentration and estradiol secretion***

305 The production of cGMP in control and treated with GPER and PPAR (alone or in
306 combinations) MA-10 cells was measured by General Cyclic guanosine monophosphate Elisa
307 kit assay (EIAab Wuhan Eiaab Science Co., LTD, Wuhan, China) according to the
308 manufacturer's instructions with detection level 0.31 to 20.0 ng/mL. The cGMP levels were
309 calculated as ng/mL.

310 Estradiol Enzyme Immunoassay Kit (DRG, Inc. Int. Springfield, USA) was used for
311 measurement of estradiol content in culture medium from control and treated with GPER and
312 PPAR (alone or in combinations) MA-10 cells according to the manufacturer's instructions.
313 The sensitivity of the assay was 10.6 pg/mL. The absorbance (λ = 450 nm) was measured.
314 Data were expressed as mean ± SD.

315 The measurements were performed with the use ELISA apparatus (Labtech LT-4500).

316 ***2.10. Statistics***

317 Three biological repeats of each sample (n = 7) and three independent experiments were
318 performed. Each variable was tested using the Shapiro-Wilk W-test for normality. The
319 homogeneity of variance was assessed with Levene's test. Comparisons were performed by
320 one-way ANOVA, followed by Dunnett's post hoc test (GB-STAT software, v. 7.0; Dynamic
321 Microsystems) to determine the significant differences between proteins expression levels,
322 and cholesterol content, cGMP content and estradiol secretion. Statistical analyses were
323 performed on raw data using Statistica 10 software (StatSoft Inc., Tulsa, OK, USA). Data
324 were presented as means ± S.D. Data were considered statistically significant at $^{*}p < 0.05$, **
325 $p < 0.01$ and $^{***}p < 0.001$.
326

327 ***Results***

328 ***3.1. Scanning electron microscopic and morphological observations of LCTs***

329 Scanning electron microscopy analyses of LCT biopsy fragments revealed the tumors are
330 relatively compact structures of oval or slightly elongated shape (Fig.1a A-C) with tumor
331 cells apposed and adhering to one another (Fig.1a D, E). It is important to note that some
332 tumor cells were fused. Our observations also revealed that compact areas of tumor cells are
333 separated by deep grooves. Between those grooves, compact tumor sheets are formed (Fig.1b
334 E-G). Cells within sheets are tightly linked by thick projections and masses of such
335 connections were observed between cells from neighboring tumor sheets (Fig.1b E –F).
336 Higher magnification revealed the presence of elongated, delicate filiform fibrillar projections
337 that form a cage-like structure covering individual tumor sheets (Fig.1b I – L).
338 Hematoxylin-eosin staining demonstrated a mixture of four types of cells in the tumor
339 mass when compared to controls, where single or small groups of Leydig cells were seen in
340 the interstitial space (Fig.2 A, B). In LCTs, most cells possessed a large polygonal shape with

abundant cytoplasm, indistinct cell borders, and regular round to oval nuclei. The nucleus was found to be frequently prominent (Fig. 2b). Occasionally, cells as those noted above were found to possess distinct cell borders and smaller nuclei (Fig. 2b'). Small cells with scant, densely eosinophilic cytoplasm and a grooved nuclei (Fig. 2b") and spindle-shaped (sarcomatoid) cells (Fig. 2b"') were observed as well.

3.2. Expression and localization of GPER and PPARs in LCTs

In LCTs, increased expression of GPER ($p < 0.05$) and decreased expression of PPARα ($p < 0.001$), PPARβ ($p < 0.01$), and PPARγ ($p < 0.001$) was seen when compared to controls (Fig.3A, B). Corresponding to GPER and PPARs protein expression changes their mRNA expressions in LCTs are presented as supplementary material (Fig.3').

No changes in GPER localization and staining intensity was found in control Leydig cells and LCTs (Fig.4 A, A'). Specifically, the staining was exclusively cytoplasmic and of moderate intensity. Localization and immunostaining intensity of PPAR varied between Leydig cells of control testis and LCTs (Fig.4B, B', C, C', D, D'). While strong cytoplasmic-nuclear expression of PPARα, β, and γ was found in control samples, an absence of PPARα expression and moderate to weak immunostaining expression of PPARβ and PPARγ, respectively, were detected. In LCTs, PPARs were located primarily in the cytoplasm of Leydig cells. No positive staining was found when primary antibodies were omitted (Fig. 4, inserts at A, D').

3.3. Expression and localization of LHR, PKA, PLIN, HSL, StAR, TSPO, HMGCS and HMGCR in LCTs

In LCTs, varying expression of LHR, PKA, PLIN, HSL, StAR, TSPO, HMGCS, and HMGCR was observed when compared to normal Leydig cells (Fig. 5A, B). The expression of LHR and PKA was increased ($p < 0.05$ and $p < 0.01$, respectively) as well as that of HMGCS and HMGCR ($p < 0.001$ and $p < 0.05$, respectively). In contrast, PLIN and StAR expression was decreased ($p < 0.001$ and $p < 0.05$, respectively), while a non-significant increase was observed for HSL and TSPO. Corresponding to LHR, PKA, PLIN, HSL, StAR, TSPO, HMGCS, and HMGCR protein expression changes their mRNA expressions in LCTs are presented as supplementary material (Fig.5').

In control Leydig cells and LCTs, cytoplasmic expression of LHR was found (Fig.6 A, A'). The immunostaining was of moderate intensity in control Leydig cells but was weak and present in minority of cells of LCTs. No differences were found in PKA distribution and immunostaining (Fig. 6 B, B'), with strong staining present in control and tumor Leydig cell cytoplasm. PLIN distribution was cytoplasmic in control Leydig cells and LCTs (Fig. 6 C, C'). In control Leydig cells, staining intensity was strong while found to be weak in LCTs. Increased HSL staining intensity was found in LCTs when compared to control cells (Fig. 6D, D') and was exclusively cytoplasmic. Strong immunoreaction was found in the blood vessel epithelium. In contrast, decreased staining intensity of StAR, exclusively present in the cytoplasm, was observed in LCTs (Fig. 6E, E') while control Leydig cells exhibited moderate cytoplasmic staining. A similar pattern was found for TSPO (Fig. 6 F, F'). Moderate cytoplasmic expression was revealed in control Leydig cell cytoplasm, while the TSPO staining intensity was very weak in LCTs. However, in a few cells immunoreaction was very strong. No differences were found in the distribution of HMGCS and HMGCR between control cells and LCTs (Fig. 6 G, G' and H, H'). Strong cytoplasmic expression of HMGCS and moderate cytoplasmic expression of HMGCR were revealed in control Leydig cells and

LCTs, respectively. No positive staining was found when primary antibodies were omitted (Fig. 4, inserts at A, F').

3.4. Effect of GPER and PPAR blockage on expression of PI3K, Akt and mTOR in LCTs

In LCTs, PI3K and Akt expression was increased ($p < 0.05$,) while no observable changes in mTOR expression was found when compared to controls (Fig. 5A, B).

3.5. Effect of GPER and PPAR blockage on cholesterol concentration, estradiol secretion and cGMP concentration in MA-10 cells

Regardless of used antagonists (alone or in combination), an increased ($p < 0.05$, $p < 0.01$) cholesterol concentration in tumor Leydig cells was seen (Fig. 8A). Secretion of estradiol markedly increased ($p < 0.001$) after GPER blockage (Fig.8B). A similar increase ($p < 0.01$) was observed after GPER and PPARα blockage. Conversely, blockage of GPER and PPARγ decreased ($p < 0.05$) estradiol secretion. When either PPARα or PPARγ was blocked, no to little alterations ($p < 0.05$) in hormone secretion were revealed.

Changes in cGMP concentration after antagonist-treatment were similar to those of estradiol secretion (Fig.8C). Treatment with a GPER antagonist, alone or in combination with a PPARα antagonist, increased ($p < 0.05$, $p < 0.01$) cGMP concentration while treatment with PPARα or γ antagonists consistently decreased ($p < 0.05$) the concentration. Only treatment with GPER and PPARγ antagonists in combination increased ($p < 0.01$) cGMP concentration.

Discussion

In the present study, we examined the cellular organization and molecular mechanisms, including GPER and PPAR signaling, lipid balance, and steroidogenesis-regulating molecular interactions that regulate LCT biology.

For the first time, scanning electron microscopic analysis was used to visualize the general organization of LCTs. We showed a complicated LCT structure where individual cells were not recognized in the solid mass, but a number of prolongations of various size were formed, keeping cells tightly linked to each other. Of note, according to Kim *et al.,* [14] and Al-Agha and Axiotis [56], benign LCTs classically present as a small (3–5 cm in diameter), sharply delineated and solid mass embedded within the testis. Alternatively, malignant LCTs are typically larger (greater than 5 cm in diameter), have infiltrative margins, and show areas of hemorrhage and necrosis. They replace the testis and/or extend beyond testicular parenchyma. Morphologically, LCTs can consist predominantly of one type or as a mixture of the four types of cells [57] observed in specimens examined herein. Pale to clear cytoplasm of LCTs, related to abundant lipid accumulation, was reported by Al-Agha and Axiotis [56]. Other characteristic frequently observed is a rich cytoplasmic lipofuscin pigment that is distinctive for LCT, although it is present in other steroid hormones-secreting tumors as well as in aging cells [3]. Additionally, Reinke crystals, both intracytoplasmic and intranuclear, are often described in LCTs. Ultrastructural studies of LCTs revealed organelle content typical for steroid-secreting cells e.g. abundant smooth endoplasmic reticulum, mitochondria with tubulovesicular cristae, and numerous lipid droplets or irregularly shaped electron-dense bodies consisting of lipid droplets and accumulated in lysosomes [58].

Leydig cell tumors are sex steroid hormone-secreting tumors with androgens produced in prepubertal children and estrogens in adults [10]. A central factor in LCT growth and progression is represented by an inadequate intratesticular balance in the androgen/estrogen ratio [59]. Sirianni *et al.,* [60] demonstrated that estrogens elicit proliferative effects in human and rodent tumor Leydig cells through an autocrine mechanism. Findings from transgenic mice revealed an increased estrogen/androgen ratio, and estrogen excess resulted in Leydig cell hyperplasia, hypertrophy, and adenomas [61]. Of note, these effects can be induced by the

action of estrogen *via* canonical estrogen receptors. Varying expression patterns of ERα and ERβ were observed in human LCTs compared to healthy testis [36]. Also, in human and rat LCTs, involvement of GPER in cell proliferation, growth, and apoptosis was shown [62]. Rago *et al.,* [63, 64] confirmed the presence of GPER in germ cell tumors and sex-cord stromal tumors. From the latter group, in LCTs, the authors found no differences in GPER expression in relation to normal testis. In contrast, we revealed an increase in GPER expression in LCTs when compared to normal Leydig cells. Moreover, in preliminary *in vitro* experiments in mouse tumor Leydig cells, GPER expression was increased [54].

Herein, we showed GPER, alone and together with PPARα, effected estradiol secretion by tumor Leydig cells, although GPER and PPAR increased cholesterol levels in these cells. Such results indicate a leading role of GPER over PPAR in regulation of sex hormone production and secretion, and it suggests possible GPER and PPARα alterations in LCTs. Similarly, our prior study also showed progesterone secretion modulation in GPER and PPAR antagonists-treated tumor mouse Leydig cells [52]. According to findings by Chimento *et al.,* [62], GPER is a good target for reduction of tumor Leydig cell proliferation. In tumor rat Leydig cells (R2C), GPER activation by its agonist (G-1) was associated with the initiation of the intrinsic apoptotic mechanism. Other experimental studies showed that endocrine disrupting chemicals, acting through GPER signaling, are involved in testicular germ cell carcinogenesis [37].

Interestingly, androgens have been shown to inhibit tumor Leydig cell proliferation by opposition to self-sufficient *in situ* estrogen production in R2C cells [46]. Androgen treatment significantly decreased the expression and activity of estrogen synthase (aromatase). This inhibitory effect relied on androgen receptor (AR) activation and involved negative regulation of the aromatase gene (*CYP19*) transcriptional activity through the nuclear orphan receptor DAX-1 (dosage-sensitive sex reversal, adrenal hypoplasia critical region, on chromosome X,

gene 1). Alternatively, the negative role of anabolic androgenic steroids in supraphysiologic dosage was recently implicated in mechanisms of tumorigenesis *via* impairment of the expression of steroidogenic enzymes and effects on intratesticular hormonal balance [65]. Of note, male patients with congenital adrenal hyperplasia (CAH) can develop bilateral testicular adrenal rest tumors (TARTs). These tumors, in most cases, regress with glucocorticoid therapy but histological differentiation from Leydig-cell tumors is quite difficult [66]. Ulbright *et al.,* [3] reported unusual features of LCTs e.g. adipose differentiation, calcification with ossification, and spindle-shaped tumor cells in both young and ageing patients. Awareness of these features may prevent misinterpretation.

Two standards are currently used to distinguish between hyperplastic nodules from adenomas. An adenoma classification is warranted if its diameter exceeds either one seminiferous tubule cross-section [67] or three seminiferous tubule cross-sections [69]. Leydig cell hyperplasia (focal or diffuse) and adenomas are commonly observed in laboratory rodents. The spontaneous incidence of adenomas in ageing Sprague-Dawley and inbred Fischer 344 rats, as well as mature CD-l and B6C3Fl mice, have been documented [68]. Morphologically, no differences appear between spontaneous or chemically induced Leydig cell adenomas [69].

Increased PPAR expression in organ pathophysiology e.g. liver, heart, intestine, and renal proximal tubules, is currently only partially elucidated [70-73]. We showed, for the first time, a PPAR expression pattern in normal human Leydig cells and its prominent down regulation in LCT. Immunoreactive PPARα and β were clearly apparent in testicular germ cell tumors [74]. A similar correlation was found in dog testis, and PPAR expression was always markedly higher in tumor tissue [75]. Recently, Kadivr *et al.,* [76] reported a relationship between PPAR mRNA expression and spermatozoa motility in rams. Notably, confusing results were seen concerning the involvement of PPAR in tumor biology. PPAR was revealed

to both promote and inhibit cancer *via* effects on cell differentiation, growth, metastasis, and lipid metabolism [77].

In our findings, both *in vivo* and *in vitro* studies revealed a partnership between GPER, PPAR, and lipid homeostasis-controlling molecules in LCT. These molecules showed altered expression patterns in relation to GPER and PPAR expression in LCT.

The effect of either GPER or PPAR on cholesterol content suggests alterations in cholesterol synthesis and/or storage that may be based on GPER and/or PPAR disturbances. Recent studies have also linked lipids abundance with increased tumor aggressiveness and its resistance to chemotherapy [78]. Wang *et al.,* [79] reported high cholesterol content and infertility in HSL knockout mice; however, no information on Leydig cell function was provided. Our studies revealed HSL expression was not disturbed in LCTs. Findings by Christian *et al.,* [80] showed that autophagy influences lipid metabolism *via* both lipogenesis (supporting cell growth within nutrient-limited areas, thereby contributing to tumor symbiotic relationships) and lipolysis. Lipid droplets may induce autophagy and undergo lipophagy to avoid lipotoxicity, a phenomenon caused by excessive lipid accumulation with involvement of the mTOR signaling pathway [81]. Thus, we show increased cholesterol content without activated mTOR can indirectly result in lipophagy induction in LCTs. It seems this particular tumor can have a distinct biology, but it is possible that some mechanisms can be induced later when its development is more advanced.

Lastly, findings by Ma *et al*., [82] demonstrated that culture of rat Leydig cells in hypoxic conditions decreased cholesterol content. These findings indicate that, besides well-known lipid homeostasis controlling molecules, a number of factors of various origin/nature are implicated in its regulation. In steroidogenic cells, the mechanism underlying lipid turnover and receptor involvement remained unanswered [77] however, based on these results, GPER-PPAR cross-talk should be taken into consideration. The question also arises whether some of

these factors and/or molecules, when disturbed, lead to Leydig cell tumorigenesis with additional perturbations in lipid homeostasis/steroidogenesis, or whether perturbations in lipid homeostasis-controlling factors/molecules occur as a result of tumor initiation and development. Based on all of the aforementioned results, both mechanisms are equally possible.

The color of LCTs usually ranges from brown to yellow to gray-white depending on the lipid content of the tumor [83]. The golden-brown appearance (usually imparted by the abundant lipofuscin pigment of tumor cells) is very characteristic. According to our results, in LCTs, lipid homeostasis is disturbed as seen for other endocrine and non-endocrine tumors [84]. Various changes were revealed in expression and localization of lipid balance-controlling molecules, including those controlling steroidogenesis as well as phosphatidylinositol-3-kinase (PI3K)-Akt-mTOR signaling pathway. Scarce data concerning lipid homeostasis and/or its controlling molecules in rodent tumor Leydig cells are available.

The steroidogenic function of Leydig cells can be modulated in various physiological conditions. *In vivo* studies in young and ageing rats revealed increased sex steroid synthesis in animals administered with a TSPO ligand (FGIN-1-27) [85]. In both age groups, serum testosterone levels increased significantly. Herein, HSL and TSPO expression did not vary in LCTs, suggesting a subordinate role of these molecules in LCTs. In the Leydig cell line (M5480), an acute effect of hCG was observed as increased metabolism of cholesteryl esters was reported [87]. Moreover, in patients with testicular cancer, hCG treatment caused excess of estradiol secretion by the tumor [88]. In a mouse tumor Leydig cell line (mLTC-1), epidermal growth factor increased StAR activity and steroid production efficiency in a time- and dose-dependent manner with involvement of ERK, while LHR expression was significantly reduced [88]. In mice (C57BL/6J) with LCTs, cessation of steroidogenesis was present when LH and cAMP were removed [89]. We found prominent changes in LHR and

PKA expression, reflecting disturbances in lipid controlling mechanisms directly associated with central endocrine regulation and the local microenvironment. For example, due to implications of HMGCR in cancer cell proliferation and cooperation with Ras signaling, HMGCR is used as a molecular target of statins, cholesterol-lowering drugs [90].

Metabolic flux and availability of lipids is controlled directly by lipid droplets and peroxisomes. These lipids serve as membrane stabilizers and structural elements, protein modifiers and signaling molecules, as well as energy sources for cell growth, migration, and invasion [91,92]. Therefore, failure of one of the lipid machinery components results in a negative effect on global cell physiology and lipid homeostasis. In pancreatic cancer, the content of lipid droplets is mobilized under a restricted cholesterol-rich, low-density lipoprotein (LDL) supply. Limiting LDL uptake reduces the oncogenic properties of this cancer and renders it more sensitive to cytotoxic drugs [93].

It is worth noting that lipid droplet associated proteins are actively involved in modulating lipid homeostasis by generating sites for steroidogenic enzyme activity [94, 95]. Marked expression changes in PLIN reflect that it can affect steroidogenic enzymes, thereby aiding in the development of LCTs. Upon stimulation of mLTC-1 cells with LH or 8-bromo-cAMP, large lipid droplets become much smaller and are dispersed throughout the cytosol. Lukyaenko *et al*., [95] demonstrated lipophilic macrophage-derived factor as a highly active, acute regulator of steroidogenesis, acting through a high capacity StAR-independent pathway.

Alterations in the mitochondrial status affect cell lipid homeostasis and steroid biosynthesis efficiency [96, 97]. Mitophagy serves as an indispensable mechanism to transfer damaged mitochondria for lysosomal degradation. In LCTs, either mitochondrial function and/or mitophagy can be altered, thus affecting lipid homoeostasis as indirectly shown through perturbations in StAR expression patterns.

564 It is worth adding that lipids have been recognized as a component of metabolic
565 reprogramming in tumor cells [98]. Many tumors show a reactivation of *de novo* fatty-acid
566 synthesis for generation of membrane structural lipids; thus, they do not rely on lipids from
567 the bloodstream [99]. Modulated lipid synthesis may also have a non-cell-autonomous role in
568 cancer development. The growth and metastasis promotion of LCT cannot be excluded with
569 participation of adipocytes [100]. In addition to their structural and signal transduction
570 roles, lipids can also be broken down into bioactive lipid mediators, regulating a variety of
571 carcinogenic processes including cell growth, cell migration, and metastasis formation, as
572 well as the uptake of chemotherapeutic drugs [101, 102]. Therefore, based on our results
573 that show alterations in various lipid-controlling molecules, further studies are needed to
574 elucidate the type, role, and regulation of lipids synthesized in tumors of steroidogenic cells.
575 In prostate cancer progression, stimulatory effect of insulin on steroidogenesis was reported
576 [103].
577 Enhanced expression of sterol regulatory element binding proteins (SREBPs), involved in
578 cholesterol and fatty acids synthesis through the Akt pathway (anchored-lipid membrane
579 protein), correlates with tumor development, progression, and invasiveness, as well as
580 increased lipid content in cell membranes [104]. Lipid raft disruption inhibits Akt
581 activation thereby reducing tumor cell proliferation [105]. The tumor microenvironment has
582 an essential role in the metabolic adaptation of cancer cells [77]. Through both the post-
583 translational regulation and induction of transcriptional programs, the dysregulated PI3K-Akt-
584 mTOR pathway coordinates the uptake and utilization of multiple nutrients e.g. lipids
585 supporting the enhanced growth and proliferation of cancer cells [106]. In the testis, blockage
586 of mTOR markedly decreased intracellular testosterone concentration [106]. In this study, we
587 found PI3K, Akt, and mTOR signaling alterations present in LCTs. It is probable that, in
588 LCTs, an increased phosphorylated and unphosphorylated kinases affect mTOR. The

589 activation of mTOR is possible by other signaling pathway or can be related to advanced LCT
590 development [107]. Our earlier studies in mouse tumor Leydig cells revealed that GPER and
591 PPAR inhibition activate PI3K and Akt [52] but mTOR is modulated diversely; inhibits by
592 GPER antagonist alone and together with PPARγ antagonist as well as activates by GPER
593 with PPARα together and the latter alone (supplementary Fig.7').

594 Distinct changes is cGMP level suggests GPER-PPAR-mediated high or only *via* PPAR
595 low metastatic activity of LCT. Besides antimetastatic strategy with cGMP against in
596 colorectal cancer metastasis cGMP as a mediator of lipolysis in bovine oocytes was confirmed
597 [108]. In LCTs, cGMP is important in maintaining lipid homeostasis when GPER and PPAR
598 are absent.

599 The outcome of lipid content modification is a result of protein–protein cross-talk between
600 messenger proteins, enzymes, and receptors that regulate pro-oncogenic and apoptotic
601 interactions, including their activity that was revealed here also between GPER-PPAR and
602 HMGCS and HMGCR resulting in overexpression of the latter enzymes that also is in line
603 with our earlier study [52]. According to Ding *et al*., [109], HMGCR is an important marker
604 for tumor testis transformation in mice.

605 Understanding the principles underlying these processes and mechanisms, as well as their
606 relationship, may provide an avenue for controlling cellular lipid balance (through
607 manipulating lipid composition), including managing post-translational modifications of
608 proteins as well as lipid-related gene expression in LCTs [110].

609 **Conclusion**

610 Mechanisms concerning Leydig cell tumorigenesis are scarce, and the role of lipid
611 metabolism in tumor cells has long been disregarded. Recently, however, these mechanisms
612 are recognized as the future of prominent target of therapy (Sreedhar and Zhao 2018).

Therefore, alterations in lipid- and cholesterol-associated proteins and mechanisms in LCTs are presented here for the first time.

Our findings shed light on the novel functional interplay between GPER and PPAR ultimately affecting lipid metabolism and steroidogenesis in LCTs. In addition, modifications of LHR, PKA, PLIN, HSL, StAR, TSPO, HMGCS, and HMGCR, together with cGMP and PI3K-Akt-mTOR pathways, may be required in developing innovating approaches (combined with transcriptome/proteome analyses and lipidomic data) that target pathological processes of Leydig cells. There is an urgent need for additional experimental and clinical data to complete the current knowledge on the biology and molecular characteristics of LCTs. Ultimately, this will guide the early diagnostics, treatment, and surveillance of incoming patients with this disease.

Author contributions

Authors' contribution to the work described in the paper: M.K-B., E.G-W., M.K., P.D., A.M., P.P., W.T., B.J. P., A.H. performed research. M.K-B., E.G-W., W.T., A.H., B.B., J.K. W. analyzed the data.

M.K.-B. designed the research study and wrote the paper. All authors have read and approved the final version of the manuscript.

Acknowledgments:

The Authors are grateful to Grzegorz Kapuscinski, FEBU (urologist) and Robert Wyban, MS (LAB-IVF) (nOvum Fertility Clinic, Warszawa) for cooperation. We thank Dr. Grzegorz Wojtczak (Department of Cell Biology and Imaging, Institute of Zoology and Biomedical Research, Jagiellonian University in Kraków) for technical help in scanning electron

microscopic analyses and to Miss Maja Kudrycka and Miss Patrycja Dutka (Department of Endocrinology) for technical help in qRT-PCR and Western blotting analyses.

Financial disclosure statement

This work was supported by a grant OPUS12 2016/23/B/NZ4/01788 (M.K-B) from National Science Centre, Poland.

Conflict of Interest: The authors declare that they have no conflict of interest.

References

1. Cheville JC. Classification and pathology of testicular germ cell and sex cord-stromal tumors. Urol Clin North Am. 1999; 26:595–609.

2. Henderson CG, Ahmed AA, Sesterhenn I, Belman AB, Rushton HG. Enucleation for prepubertal leydig cell tumor. J Urol. 2006; 176: 703–705.

3. Emerson RE, Ulbright TM. Morphological approach to tumours of the testis and paratestis. J Clin Pathol. 2007; 60: 866–880.

4. Farkas LM, Székely JG, Pusztai C, Baki M. High frequency of metastatic Leydig cell testicular tumours. Oncology. 2000; 59: 118-121.

5. Gheorghisan-Galateanu AA. Leydig cell tumors of the testis: a case report. BMC Res Notes. 2014; 7: 656.

6. Bertram KA, Bratloff B, Hodges GF, Davidson H. Treatment of malignant Leydig cell tumor. Cancer. 1991; 68, 2324–2329.

7. Rich MA, Keating MA. Leydig cell tumors and tumors associated with congenital adrenal hyperplasia. Urol Clin North Am. 2000; 27: 519–528.

8. Gana BM, Windsor PM, Lang S, Macintyre J, Baxby K. Leydig cell tumor. Br J Urol. 1995; 75: 676-678.

9. Lai N, Zeng X, Li M, Shu J. Leydig cell tumor with lung metastasis diagnosed by lung biopsy. Int J Clin Exp Pathol. 2015; 8: 12972–12976.

10. Laguna MP, Nicolai N, Oldenburg J; European Association of Urology. Guidelines on Testicular Cancer: 2015 Update. Eur Urol. 2015; 68:1054-1068.

11. Lejeune H, Habert R, Saez JM. Origin, proliferation and differentiation of Leydig cells. J Mol Endocrinol. 1998; 20: 1–25.

12. Huang Y, Song J, Xu M, Zan Q. Primary Leydig cell tumour of epididymis: a rare case report with review of literature. Andrologia. 2013; 45: 430–433.

13. Hekimgil M, Altay B, Yakut BD, Soydan S, Ozyurt C, Killi R. Leydig cell tumor of the testis: comparison of histopathological and immunohistochemical features of three azoospermic cases and one malignant case. Pathol Int. 2001; 51: 792-796.

14. Kim I, Young RH, Scully RE. Leydig cell tumors of the testis. A clinicopathological analysis of 40 cases and review of the literature. Am J Surg Pathol. 1985; 3: 177-192.

15. Tiwari P, Goel A, Sharma P, Kumar S, Vijay M, Dutta A. Leydig cell tumor with mediastinal and lung metastasis. Saudi J Kidney Dis Transpl. 2011; 22: 354-356.

16. Bozzini G, Ratti D, Carmignani L; en representación de Young Academic Urologists (YAU) Men's Health Group. Treatment of leydig cell tumours of the testis: Can testis-sparing surgery replace radicalorchidectomy? Results of a systematic review. Actas Urol Esp. 2017; 41, 146-154.

17. Giacaglia LR, Kohek MB da F, Carvalho FM, Fragoso MC, Mendonca B, Latronico AC. No evidence of somatic activating mutations on gonadotropin receptor genes in sex cord stromal tumors. Fertil Steril; 2000; 74: 992–995.

18. Carvajal-Carmona LG, Alam NA, Pollard PJ, Jones AM, Barclay E, Wortham N, et al., Adult leydig cell tumors of the testis caused by germline fumarate hydratase mutations. J Clin Endocrinol Metab. 2006; 91, 3071–3075.

19. Skakkebaek NE, Rajpert-De Meyts E, Main KM. Testicular dysgenesis syndrome: an increasingly common developmental disorder with environmental aspects. Hum Reprod. 2001; 5: 972-978.

20. Joensen UN, Jørgensen N, Rajpert-De Meyts E, Skakkebaek NE. Testicular dysgenesis syndrome and Leydig cell function. Basic Clin Pharmacol Toxicol. 2008; 102: 155-161.

21. Holm M, Rajpert-De Meyts E, Andersson AM, Skakkebaek NE. Leydig cell micronodules are a common finding in testicular biopsies from men with impaired spermatogenesis and are associated with decreased testosterone/LH ratio. J Pathol. 2003; 199: 378-386.

22. Ho GT, Gardner H, Mostofi K, DeWolf WC, Loughlin KR, Morgentaler A. The effect of testicular nongerm cell tumors on local spermatogenesis. Fertil Steril. 1994; 62: 162-166.

23. Lardone MC, Piottante A, Valdevenito R, Ebensperger M, Castro A. Histological and hormonal testicular function in oligo/azoospermic infertile men. Andrologia. 2013; 45, 379-385.

24. Kozina V, Geist D, Kubinová L, Bilić E, Karnthaler HP, Waitz T, et al., Visualization of Reinke's crystals in normal and cryptorchid testis. Histochem Cell Biol. 2011; 135: 215-228.

719 25. Soerensen RR, Johannsen TH, Skakkebaek NE, Rajpert-De Meyts E. Leydig cell
720 clustering and Reinke crystal distribution in relation to hormonal function in adult patients
721 with testicular dysgenesis syndrome (TDS) including cryptorchidism. Hormones (Athens).
722 2016; 15: 518-526.
723
724 26. Paniagua R, Nistal M, Bravo MP. Leydig cell types in primary testicular disorders. Hum
725 Pathol. 1984; 15: 181-190.
726
727 27. Zimmerli UU, Hedinger CE. Hyperplasia and hypertrophy of Leydig cells associated with
728 testicular germ cell tumours containing syncytiotrophoblastic giant cells. Virchows Arch A
729 Pathol Anat Histopathol. 1991; 419: 469-474.
730
731 28. Dirami G, Teerds KJ, Cooke BA. Effect of a dopamine agonist on the development of
732 Leydig cell hyperplasia in Sprague-Dawley rats. Toxicol Appl Pharmacol. 1996; 141, 169-
733 177.
734
735 39. Greaves P. Histopathology of preclinical toxicity studies : interpretation and relevance in
736 drug safety evaluation. 4th ed. Amsterdam: Elsevier AP. 2012; p.1-867.
737
738 30. Cook JC, Klinefelter GR, Hardisty JF, Sharpe RM, Foster PM. Rodent Leydig cell
739 tumorigenesis: a review of the physiology, pathology, mechanisms, and relevance to humans.
740 Crit Rev Toxicol. 1999; 2: 169-261.
741
742 31. Gould ML, Hurst PR, Nicholson HD. The effects of oestrogen receptors alpha and beta
743 on testicular cell number and steroidogenesis in mice. Reproduction. 2007; 134: 271-279.
744
745 32. Kotula-Balak M, Hejmej A, Kopera I, Lydka M, Bilinska B. Prenatal and neonatal
746 exposure to flutamide affects function of Leydig cells in adult boar. Domest Anim
747 Endocrinol. 2012; 42: 142-154.
748
749 33. Pawlicki P, Milon A, Zarzycka M, Galas J, Tworzydlo W, Kaminska A, et al., Does
750 signaling of estrogen-related receptors affect structure and function of bank vole Leydig cells?
751 J Physiol Pharmacol. 2017; 68: 459-476.
752
753 34. Tazi MF, Mellas S, El Fassi MJ, Farih MH. Leydig cell hyperplasia revealed by
754 gynecomastia. Rev Urol. 2008; 10: 164-167.
755
756 35. Carpino A, Rago V, Pezzi V, Carani C, Andò S. Detection of aromatase and estrogen
757 receptors (ERalpha, ERbeta1, ERbeta2) in human Leydig cell tumor. Eur J Endocrinol. 2007;
758 2: 239-244.
759
760 36. Chimento A, Sirianni R, Casaburi I, Pezzi V. GPER Signaling in Spermatogenesis and
761 Testicular Tumors. Front Endocrinol (Lausanne). 2014; 6: 30.
762
763 37. Kotula-Balak M, Milon A, Pawlicki P, Opydo-Chanek M, Galas J, Pacwa A, et al.,
764 Diverse role of estrogen-related receptors α, β and γ in biology of tumor Leydig cell. Tissue
765 Cell. 2018a; 52: 78-91.
766

767 38. Fietz D, Ratzenböck C, Hartmann K, Raabe O, Kliesch S, Weidner W, Klug J, Bergmann
768 M. Expression pattern of estrogen receptors α and β and G-protein-coupled estrogen receptor
769 1 in the human testis. Histochem Cell Biol. 2014; 142: 421-432.
770
771 39. Fietz D, Bergmann M, Hartmann K. In Situ Hybridization of Estrogen Receptors α and β
772 and GPER in the Human Testis. Methods Mol Biol. 2016; 1366: 189-205.
773
774 40. Levin ER. Minireview: extranuclear steroid receptors: roles in modulation of cell
775 functions. Mol Endocrinol. 2011; 25: 377-384.
776
777 41. Schmidt A, Endo N, Rutledge SJ, Vogel R, Shinar D, Rodan GA. Identification of a new
778 member of the steroid hormone receptor superfamily that is activated by a peroxisome
779 proliferator and fatty acids. Mol Endocrinol. 1992; 6: 1634–1641.
780
781 42. Braissant O, Foufelle F, Scotto C, Dauça M, Wahli W. Differential expression of
782 peroxisome proliferator-activated receptors (PPARs): tissue distribution of PPAR-alpha, -
783 beta, and -gamma in the adult rat. Endocrinology. 1996; 137: 354-366.
784
785 43. Harada Y, Tanaka N, Ichikawa M, Kamijo Y, Sugiyama E, Gonzalez FJ, et al., PPARα-
786 dependent cholesterol/testosterone disruption in Leydig cells mediates 2,4-
787 dichlorophenoxyacetic acid-induced testicular toxicity in mice. Arch Toxicol. 2016; 90: 3061-
788 3071.
789
790 44. Biegel LB, Hurtt ME, Frame SR, O'Connor JC, Cook JC. Mechanisms of extrahepatic
791 tumor induction by peroxisome proliferators in male CD rats. Toxicol Sci. 2001; 1: 44-55.
792
793 45. Hess RA. Estrogen in the adult male reproductive tract: A review. Reprod Biol
794 Endocrinol. 2003; 1: 52.
795
796 46. Maris P, Campana A, Barone I, Giordano C, Morelli C, Malivindi R, et al., Androgens
797 inhibit aromatase expression through DAX-1: insights into the molecular link between
798 hormone balance and Leydig cancer development. Endocrinology. 2015; 4: 1251-1262.
799
800 47. Seyfried TN, Shelton LM. Cancer as a metabolic disease. Nutr Metab. 2010; 27: 7.
801
802 48. Miller WL. A brief history of adrenal research: steroidogenesis - the soul of the adrenal.
803 Mol Cell Endocrinol. 2013; 22: 5-14.
804
805 49. Liu TF, Tang JJ, Li PS, Shen Y, Li JG, Miao HH, Li BL, Song BL. Ablation of gp78 in
806 liver improves hyperlipidemia and insulin resistance by inhibiting SREBP to decrease lipid
807 biosynthesis. Cell Metab. 2012; 8: 213-225.
808
809 50. Ascoli M. Characterization of several clonal lines of cultured Leydig tumor cells:
810 gonadotropin receptors and steroidogenic responses. Endocrinology. 1981; 108: 88–95.
811
812 52. Gorowska-Wojtowicz E, Dutka P, Kudrycka M, Pawlicki P, Milon A, Plachno B.J, et al.,
813 Regulation of steroidogenic function of mouse Leydig cells: G-coupled membrane estrogen
814 receptor and peroxisome proliferator-activated receptor partnership. J Physiol Pharmacol.
815 2018; 69: xx-xx.
816

817 53. Kotula-Balak M, Chojnacka K, Hejmej A, Galas J, Satola M, Bilinska B. Does 4-tert-
818 octylphenol affect estrogen signaling pathways in bank vole Leydig cells and tumor mouse
819 Leydig cells in vitro? Reprod Toxicol. 2013; 39: 6-16.
820
821 54. Kotula-Balak M, Pawlicki P, Milon A, Tworzydlo W, Sekula M, Pacwa A, et al., The role
822 of G-protein-coupled membrane estrogen receptor in mouse Leydig cell function-in vivo and
823 in vitro evaluation. Cell Tissue Res 2018b, doi: 10.1007/s00441-018-2861-7.
824
825 55. Smolen AJ. Image analytic techniques for quantification of immunocytochemical staining
826 in the nervous system. Conn PM. (Ed.), Methods Neurosci Acad Press, San Diego 1999; pp.
827 208–229.
828
829 56. Al-Agha OM, Axiotis CA. An in-depth look at Leydig cell tumor of the testis. Arch
830 Pathol Lab Med. 2007; 131: 311–317.
831
832 57. Richmond I, Banerjee SS, Eyden BP, Sissons MC. Sarcomatoid Leydig cell tumor of the
833 testis. Histopathology. 1995; 27: 578–580.
834
835 58. Ghadially FN. Ultrastructural Pathology of the Cell and Matrix. 4th ed. Boston, Mass:
836 Butterworth-Heinemann; 1997.
837
838 59. Carreau S, Wolczynski S, Galeraud-Denis I. Aromatase, oestrogens and human male
839 reproduction. Philos Trans R Soc Lond B Biol Sci. 2010; 365: 1571–1579.
840
841 60. Sirianni R, Chimento A, Malivindi R, Mazzitelli I, Andò S, Pezzi V. Insulin-like growth
842 factor-I, regulating aromatase expression through steroidogenic factor 1, supports estrogen-
843 dependent tumor Leydig cell proliferation. Cancer Res. 2007; 67: 8368 – 8377.
844
845 61. Fowler KA, Gill K, Kirma N, Dillehay DL, Tekmal RR. Overexpression of aromatase
846 leads to development of testicular leydig cell tumors: an in vivo model for hormone-mediated
847 testicular cancer. Am J Pathol. 2000; 156: 347–353.
848
849 62. Chimento A, Casaburi I, Bartucci M, Patrizii M, Dattilo R, Avena P, et al., Selective
850 GPER activation decreases proliferation and activates apoptosis in tumor Leydig cells. Cell
851 Death Dis. 2011; 1: 4:e747.
852
853 63. Rago V, Romeo F, Giordano F, Ferraro A, Ando S, Carpino A. Identification of ERbeta1
854 and ERbeta2 in human seminoma, in embryonal carcinoma and in their adjacent intratubular
855 germ cell neoplasia. Reprod Biol Endocrinol. 2009; 7:56.10.1186/1477-7827-7-56.
856
857 64. Rago V, Romeo F, Giordano F, Maggiolini M, Carpino A. Identification of the estrogen
858 receptor GPER in neoplastic and non-neoplastic human testes. Reprod Biol Endocrinol.
859 20111; 9:135.10.1186/1477-7827-9-135.
860
861 65. Salerno M, Cascio O, Bertozzi G, Sessa F, Messina A, Monda V, et al., Anabolic
862 androgenic steroids and carcinogenicity focusing on Leydig cell: a literature review.
863 Oncotarget. 2018; 10: 19415-19426.
864

865 66. Altieri VM, Altieri B, Castellucci R, Alba S, Bottone F, Fragalà E, et al., Leydig cell
866 tumour and giant adrenal myelolipoma associated with adrenogenital syndrome: a case report
867 with a review of the literature. Urologia. 2016; 83: 43-48.
868
869 67 .BOOmIan GA, Eustis SL, Elwell MR, Montgomery CA, MacKenzie WF, (eds.)
870 Pathology of the Fischer rat: Reference and atlas. San Diego: Academic Press; 1990.
871
872 68. McConnell RF, Westen HH, Ulland BM, Bosland MC, Ward JM. Proliferative lesions of
873 the testes in rats with selected examples from mice. URG-3, Guides for toxicologic pathology,
874 STP/ARP/AFIP, Washington; 1992.
875
876 69. Clegg ED, Cook JC, Chapin RE, Foster PM, Daston GP. Leydig cell hyperplasia and
877 adenoma formation: mechanisms and relevance to humans. Reprod Toxicol. 1997; 11: 107-
878 121.
879
880 70. Rasoulpour RJ, Terry C, LeBaron MJ, Stebbins K, Ellis-Hutchings RG, Billington R.
881 Mode-of-action and human relevance framework analysis for rat Leydig cell tumors
882 associated with sulfoxaflor. Crit Rev Toxicol. 2014; 2: 25-44.
883
884 71. Aoyama T, Peters JM, Iritani N, Nakajima T, Furihata K, Hashimoto T, et al., Altered
885 constitutive expression of fatty acid-metabolizing enzymes in mice lacking the
886 peroxisomeproliferator-activated receptor alpha (PPARalpha). J Biol Chem. 1998; 273:
887 5678-5684.
888
889 72. Watanabe K, Fujii H, Takahashi T, Kodama M, Aizawa Y, Ohta Y, et al., Constitutive
890 regulation of cardiac fatty acid metabolism through peroxisome proliferator-activated receptor
891 alpha associated with age-dependent cardiac toxicity. J Biol Chem. 2000; 29: 22293-22299.
892
893 73. Kamijo Y, Hora K, Tanaka N, Usuda N, Kiyosawa K, Nakajima T, et al., Identification of
894 functions of peroxisome proliferator-activated receptor alpha in proximal tubules. J Am Soc
895 Nephrol. 2002; 13: 1691- 1702.
896
897 74. Hase T, Yoshimura R, Mitsuhashi M, Segawa Y, Kawahito Y, Wada S, et al., Expression
898 of peroxisome proliferator-activated receptors in human testicular cancer and
899 growthinhibition by its agonists. Urology. 2002; 60: 542-547.
900
901 75. Sozmen M, Kabak YB, Gulbahar MY, Gacar A, Karayigit MO, Guvenc T, et al.,
902 Immunohistochemical characterization of peroxisome proliferator-activated receptors in
903 canine normal testis and testicular tumours. J Comp Pathol. 2013; 149: 10-18.
904
905 76. Kadivar A, Heidari Khoei H, Hassanpour H, Ghanaei H, Golestanfar A, Mehraban H, et
906 al., Peroxisome proliferator-activated receptors (PPARα, PPARγ and PPARβ/δ) gene
907 expression profile on ram spermatozoa and their relation to the sperm motility. Vet Res
908 Forum. 2016; 7: 27-34.
909
910 77. Maan M, Peters JM2, Dutta M3, Patterson AD. Lipid metabolism and lipophagy in
911 cancer. Biochem Biophys Res Commun. 2018; 10, pii: S0006-291X(18)30326-7.
912
913 78. Tirinato L, Pagliari F, Limongi T, Marini M, Falqui A, Seco J, et al., An Overview of
914 Lipid Droplets in Cancer and Cancer Stem Cells. Stem Cells Int. 2017:1656053.

79. Wang F, Chen Z, Ren X, Tian Y, Wang, Liu C, et al., Hormone-sensitive lipase deficiency alters gene expression and cholesterol content of mousetestis. Reproduction. 2017; 2:175-185.

80. Christian P, Sacco J, Adeli K. Autophagy: Emerging roles in lipid homeostasis and metabolic control. Biochim Biophys Acta. 2013; 1831: 819–824.

81. Yang M, Zhang Y, Ren J. Autophagic Regulation of Lipid Homeostasis in Cardiometabolic Syndrome. Front Cardiovasc Med. 2018; 3: 38.

82. Ma Y, Zhou Y, Zhu YC, Wang SQ, Ping P, Chen XF. Lipophagy Contributes to Testosterone Biosynthesis in Male Rat Leydig Cells. Endocrinology. 2018; 2: 1119-1129.

83. Maizlin ZV, Belenky A, Kunichezky M, Sandbank J, Strauss S. Leydig cell tumors of the testis: gray scale and color Doppler sonographic appearance. J Ultrasound Med. 2004; 23: 959-964.

84. Ishii T, Fukuzawa R, Sato T, Muroya K, Adachi M, Ihara K, et al., Gonadal macrophage infiltration in congenital lipoid adrenal hyperplasia. Eur J Endocrinol. 2016; 175: 127-132.

85. Chung JY, Chen H, Midzak A, Burnett AL, Papadopoulos V, Zirkin BR. Drug ligand-induced activation of translocator protein (TSPO) stimulates steroid production by aged brown Norway rat Leydig cells. Endocrinology. 2013; 154: 2156-2165.

86. Albert DH, Ascoli M, Puett D, Coniglio JG. Lipid composition and gonadotropin-mediated lipid metabolism of the M5480 murine Leydig celltumor. J Lipid Res. 1980; 21: 862-867.

87. Morrish DW, Venner PM, Siy O, Barron G, Bhardwaj D, Outhet D. Mechanisms of endocrine dysfunction in patients with testicular cancer. J Natl Cancer Inst. 1990; 82: 412-418.

88. Manna PR, Jo Y, Stocco DM. Regulation of Leydig cell steroidogenesis by extracellular signal-regulated kinase 1/2: role of protein kinase A and protein kinase C signaling. J Endocrinol. 2007; 193: 53-63.

89. Moyle WR, Moudgal NR, Greep RO. Cessation of steroidogenesis in Leydig cell tumors after removal of luteinizing hormone and adenosine cyclic 3',5'-monophosphate. J Biol Chem. 1971; 16: 4978-4982.

90. Basharat P, Arash H, Lahouti AH, Paik JJ, Albayda J, Pinal-Fernandez I, et al., Statin-induced Anti-HMGCR-associated Myopathy. J Am Coll Cardiol. 2016; 68: 234–235.

91. Baba Y, Funakoshi T, Mori M, Emoto K, Masugi Y, Ekmekcioglu S, et al., Expression of monoacylglycerol lipase as a marker of tumour invasion and progression in malignant melanoma. J Eur Acad Dermatol Venereol. 2017; 31: 2038-2045.

92. Hanahan D, Weinberg RA. Hallmarks of cancer: the next generation. Cell. 2011; 144: 646–674.

93. Yamaguchi T, Fujikawa N, Nimura S, Tokuoka Y, Tsuda S, Aiuchi T, et al., Characterization of lipid droplets in steroidogenic MLTC-1 Leydig cells: Protein profiles and the morphological change induced by hormone stimulation. Biochim Biophys Acta. 2015; 1851: 1285-1295.

94. Shen WJ, Azhar S, Kraemer FB. Lipid droplets and steroidogenic cells. Exp Cell Res. 2016; 15: 209-214.

95. Lukyanenko YO, Carpenter AM, Brigham DE, Stocco DM, Hutson JC. Regulation of Leydig cells through a steroidogenic acute regulatory protein-independent pathwayby a lipophilic factor from macrophages. J Endocrinol. 1998; 158: 267-275

96. Allen JA, Shankara T, Janus P, Buck S, Diemer T, Hales KH, et al., Energized, polarized, and actively respiring mitochondria are required for acute Leydig cellsteroidogenesis. Endocrinology. 2006; 147: 3924-3935.

97. Barbosa AD, Siniossoglou S. Function of lipid droplet-organelle interactions in lipid homeostasis. Biochim Biophys Acta. 2017; 1864: 1459-1468.

98. Schulze A, Harris AL. How cancer metabolism is tuned for proliferation and vulnerable to disruption. Nature. 2012; 491: 364-73.

99. Baenke F, Peck B, Miess H, Schulze A. Hooked on fat: the role of lipid synthesis in cancer metabolism and tumour development. Dis Model Mech. 2013; 6: 1353–1363.

100. Luo X, Cheng C, Tan Z, Li N, Tang M, Yang L, et al., Emerging roles of lipid metabolism in cancer metastasis. Mol Cancer. 2017; 16: 76.

101. Barrera G. Oxidative stress and lipid peroxidation products in cancer progression and therapy. ISRN Oncol. 2012; 137289.

102. Mostaghel EA, Nelson PS. Intracrine androgen metabolism in prostate cancer progression: mechanisms of castration resistance and therapeutic implications. Best Pract Res Clin Endocrinol Metab. 2008; 22: 243–258.

103. Bao J, Zhu L, Zhu Q, Su J, Liu M, Huang W. SREBP-1 is an independent prognostic marker and promotes invasion and migration in breast cancer. Oncol Lett. 2016; 12: 2409–2416.

104. Beloribi-Djefaflia S, Vasseur S, Guillaumond F. Lipid metabolic reprogramming in cancer cells. Oncogenesis. 2016; 25, e189.

105. Follo MY, Manzoli L, Poli A, McCubrey JA, Cocco L. PLC and PI3K/Akt/mTOR signalling in disease and cancer. Adv Biol Regul. 2015; 57: 10-16.

106. Oliveira PF, Cheng CY, Alves MG. Emerging Role for Mammalian Target of Rapamycin in Male Fertility. Trends Endocrinol Metab. 2017; 28: 165-167.

107. Mendoza MC, Er EE, Blenis J. The Ras-ERK and PI3K-mTOR pathways: cross-talk and compensation. Trends Biochem Sci. 2011; 36: 320-328.

108. Schwarz KRL, de Castro FC, Schefer L, Botigelli RC, Paschoal DM, Fernandes H, et al., The role of cGMP as a mediator of lipolysis in bovine oocytes and its effects on embryo development and cryopreservation. PLoS One 2018; 13: e0191023.

109. Ding J, Jiang D, Kurczy M, Nalepka J, Dudley B, Merkel EI, et al., Inhibition of HMG CoA reductase reveals an unexpected role for cholesterol during PGC migration in the mouse. BMC Dev Biol. 2008; 31: 120.

110. Audagnotto M, Del Peraro M. Protein post-translational modifications: In silico prediction tools and molecular modeling. Comput Struct Biotechnol J. 2017; 15: 307–319.

Figure captures

Figure 1. Morphology of human Leydig cell tumors – scanning electron microscopic analysis

(1a A-F and 1b G-L) Representative microphotographs of scanning electron microscopic analysis of human Leydig cell tumors (LCTs). Bars represent 1µm. For analysis n = 12 specimens were used.

Figure 2. Morphology of human Leydig cell tumors – hematoxylin-eosin staining

Representative microphotographs of (A) control human testis and (B, b-b’’’) Leydig cell tumors (LCTs). Scale bars represent 15 µm. Staining was performed on serial testicular sections from n = 12 specimens.

LC- Leydig cells, EC - epithelial cells of blood vessels

(b) - arrows depict cells of large polygonal shape with abundant, cytoplasm, indistinct cell borders, and regular, round to oval nuclei. Prominent nucleus visible at (b) higher magnification (arrowheads), (b’) - arrows depict cells with above features but possessing distinct cell borders and smaller nuclei, (b’’) - arrows depict small cells with scant, densely eosinophilic cytoplasm and grooved nuclei, (b’’’) – arrows depict spindle-shaped (sarcomatoid) cells.

Figure 3. Expression of GPER, PPARα, PPARβ and PPARγ in human Leydig cell tumor.

(A) Representative blots of qualitative expression of GPER, PPARα, and PPARγ and (B) relative expression (relative quantification of protein density (ROD); arbitrary units). The relative amount of respective proteins normalized to β-actin. ROD from three separate analyses is expressed as means ± SD. Asterisks show significant differences between respective control and Leydig cell tumor (LCTs). Values are denoted as $^{*}p < 0.05$, $^{**}p < 0.01$ and $^{***}p < 0.001$. Analysis was performed in triplicate (n = 7).

Figure 3' Expression of GPER, PPARα, PPARβ and PPARγ mRNA in human Leydig cell tumor.

Relative level (relative quantification; RQ) of mRNA for **GPER, PPARα, PPARβ and PPARγ** determined using real-time RT-PCR analysis $2^{-\Delta Ct}$ method. As an intrinsic control, β-actin mRNA level was measured in the samples. RQ from three separate analyses is expressed as means ± SD. Asterisks show significant differences between respective control and Leydig cell tumor (LCTs). Values are denoted as $^{*}p < 0.05$, and $^{***}p < 0.001$. Analysis was performed in triplicate (n = 7).

Figure 4. Localization of GPER, PPARα, PPARβ and PPARγ in human Leydig cell tumor.

Representative microphotographs of cellular localization of GPER (A, A'), PPARα (B, B'), PPARβ (C, C') and PPARγ (D, D' and higher magnification at D) in control human testes (A-

D and higher magnification at D) and Leydig cell tumor (LCTs). DAB immunostaining with hematoxylin counterstaining. Scale bars represent 15 μm. Staining was performed on serial testicular sections from n = 12 specimens.

Arrows depict cytoplasmic staining, arrowheads depict nuclear staining. No positive staining is seen when the primary antibodies were omitted – insert at A and D'-(negative controls).

Figure 5. Expression of LHR, PKA, PLIN, HSL, StAR, TSPO, HMGCS and HMGCR in human Leydig cell tumor.

(A) Representative blots of qualitative expression of LHR, PKA, PLIN, HSL, PLIN, StAR, TSPO, HMGCS and HMGCR and (B) relative expression (relative quantification of protein density (ROD); arbitrary units). The relative amount of respective proteins normalized to β-actin. ROD from three separate analyses is expressed as means ± SD. Asterisks show significant differences between respective control and Leydig cell tumor (LCTs). Values are denoted as * $p < 0.05$, ** $p < 0.01$ and $^{***}p < 0.001$. Analysis was performed in triplicate (n = 7).

Figure 5' Expression of LHR, PKA, PLIN, HSL, PLIN, StAR, TSPO, HMGCS and HMGCR mRNA in human Leydig cell tumor.

Relative level (relative quantification; RQ) of mRNA for LHR, PKA, PLIN, HSL, PLIN, StAR, TSPO, HMGCS and HMGCR determined using real-time RT-PCR analysis $2^{-\Delta Ct}$ method. As an intrinsic control, β-actin mRNA level was measured in the samples. RQ from three separate analyses is expressed as means ± SD. Asterisks show significant differences between respective control and Leydig cell tumor (LCTs). Values are denoted as * $p < 0.05$, ** $p < 0.01$ and $^{***}p < 0.001$. Analysis was performed in triplicate (n = 7).

Figure 6. Localization of LHR, PKA, PLIN, HSL, StAR, TSPO, HMGCS and HMGCR in human Leydig cell tumor.

Representative microphotographs of cellular localization of LHR (A-A'), PKA (B-B'), PLIN(C-C' and higher magnifications at C and C'), HSL (D-D'), StAR (E-E'), TSPO (F-F'), HMGCS (G-G') and HMGCR (H-H') in control human testes (A-H and higher magnification at C) and Leydig cell tumor (A'-H' and higher magnification at C'). DAB immunostaining with hematoxylin counterstaining. Scale bars represent 15 μm. Staining was performed on serial testicular sections from n = 12 specimens. Arrows depict cytoplasmic staining. Arrowheads depict strong stained cells for TSPO and positively stained epithelial cells of blood vessels for HSL. No positive staining is seen when the primary antibodies were omitted – insert at A and F'-(negative controls).

Figure 7. Expression of PI3K-Akt-mTOR pathway in human Leydig cell tumor.

(A) Representative blots of qualitative expression of PI3K, Akt, mTOR and (B) relative expression (relative quantification of protein density (ROD); arbitrary units). The relative amount of respective proteins normalized to β-actin. ROD from three separate analyses is expressed as means ± SD. Asterisks show significant differences between control and Leydig cell tumor (LCTs). Values are denoted as * $p < 0.05$. Analysis was performed in triplicate (n = 7).

Figure 7' (supplementary). Effect of GPER and PPAR blockage on expression of mTOR in MA-10 cells

(A) Representative blots of qualitative expression of mTOR and (B) relative expression (relative quantification of protein density (ROD); arbitrary units). The relative amount of

protein normalized to β-actin. ROD from three separate analyses is expressed as means ± SD. Asterisks show significant differences between control and treated Leydig cells. Values are denoted as $^{*}p < 0.05$, $^{**}p < 0.01$ and $^{***}p < 0.001$. Analysis was performed in triplicate (n = 3 for each experimental group).

Figure 8. Effect of GPER and PPAR blockage on expression on cholesterol content, estradiol secretion and cGMP concentration in MA-10 cells

Cholesterol content (A), estradiol secretion (B) and cGMP concentration (C) in control and treated with GPER (10nM), PPARα (10μM) and PPARγ (μM) antagonists alone or in combinations for 24h tumor mouse Leydig cells (MA-10). Asterisks show significant differences between control and treated Leydig cells. Values are denoted as $^{*}p < 0.05$, $^{**}p < 0.01$ and $^{***}p < 0.001$. Analysis was performed in triplicate (n = 3 for each experimental group).

1a

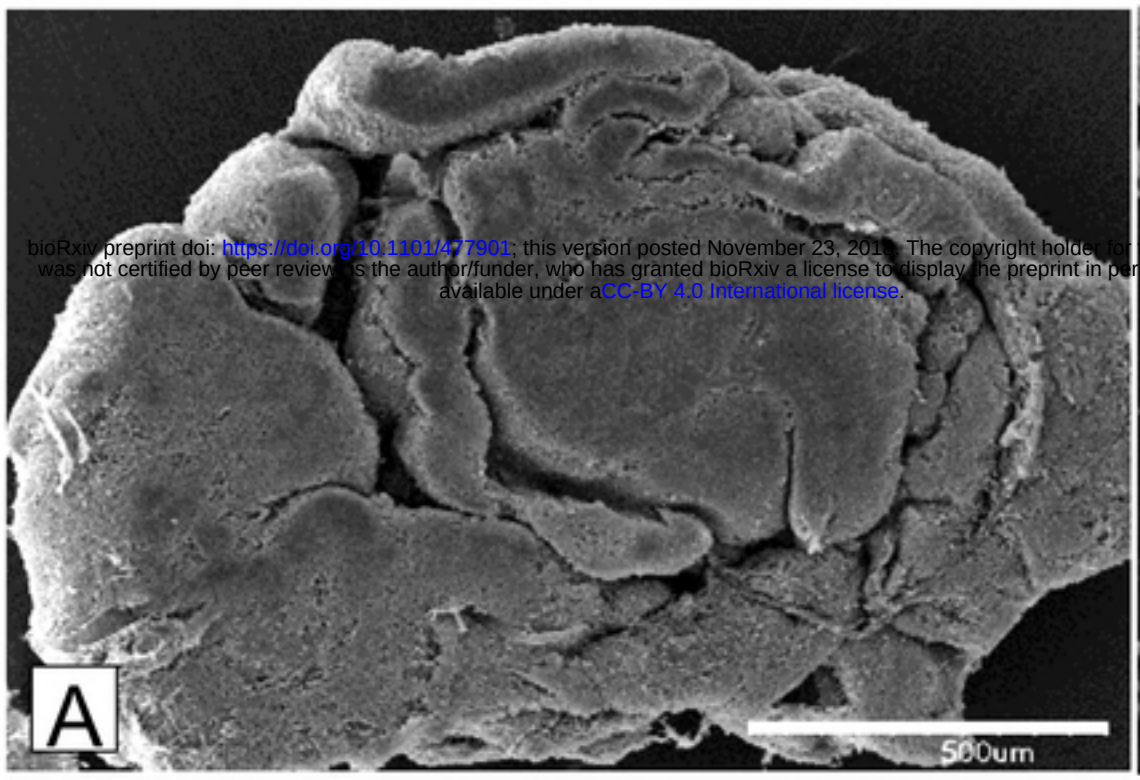

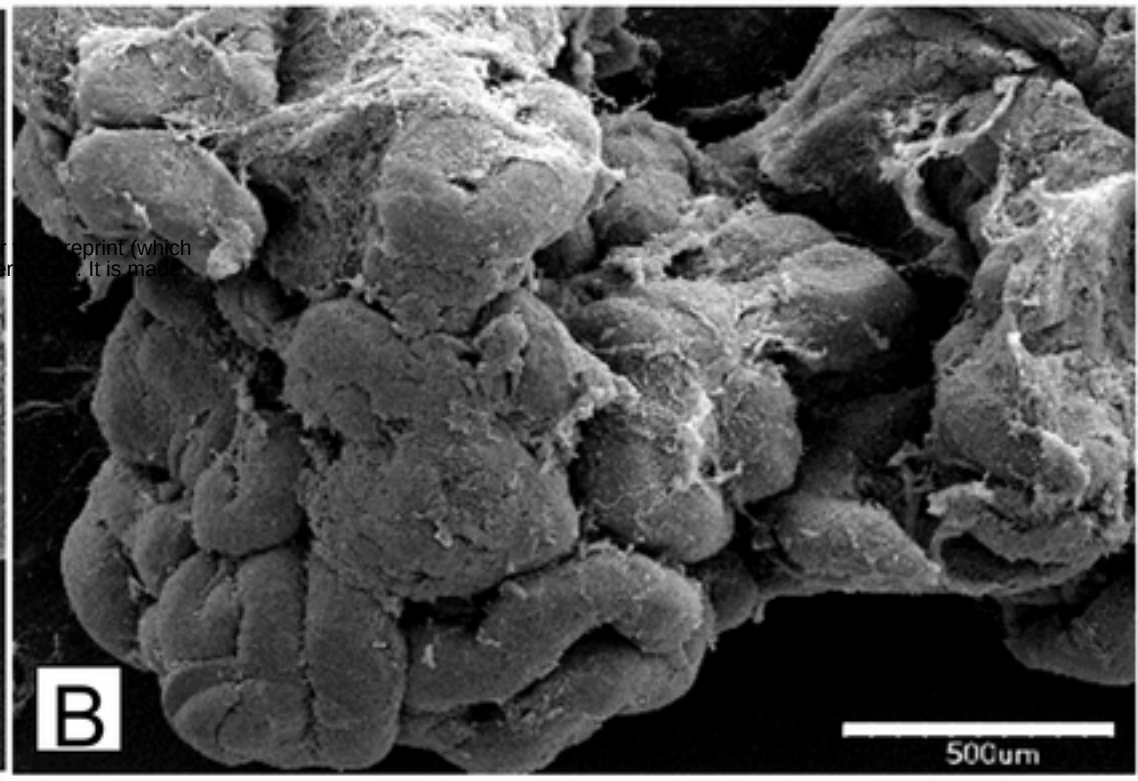

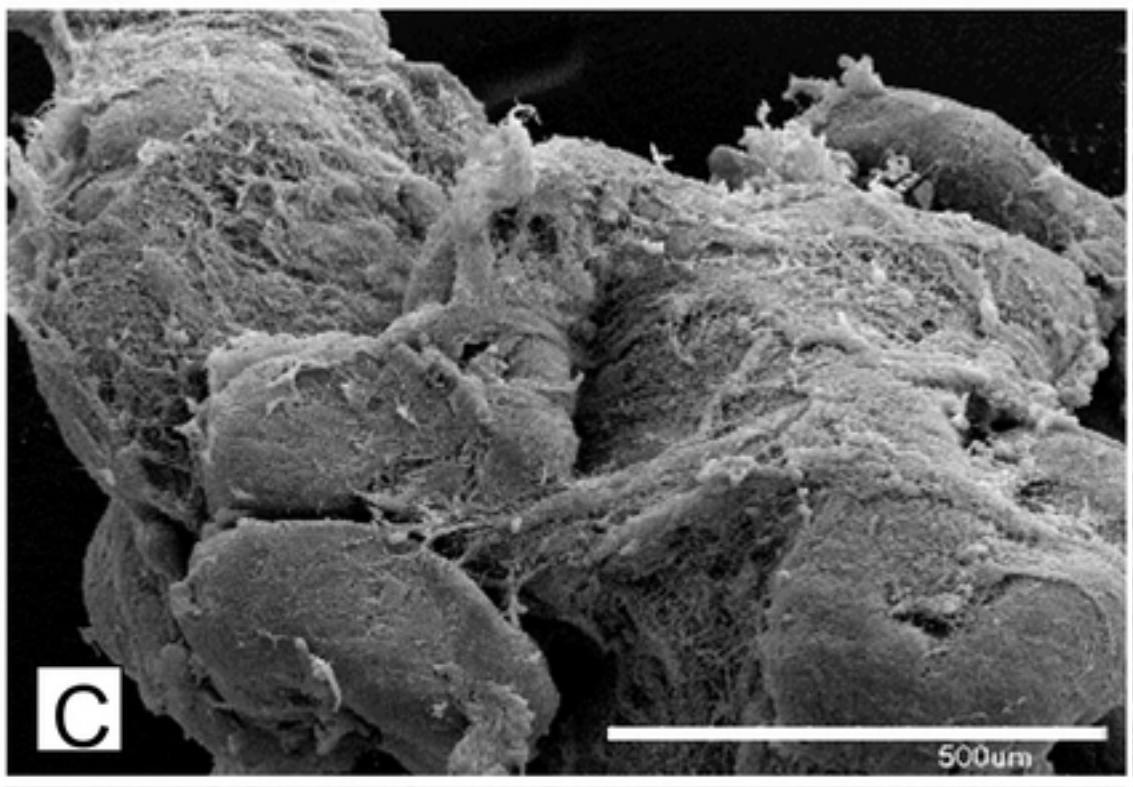

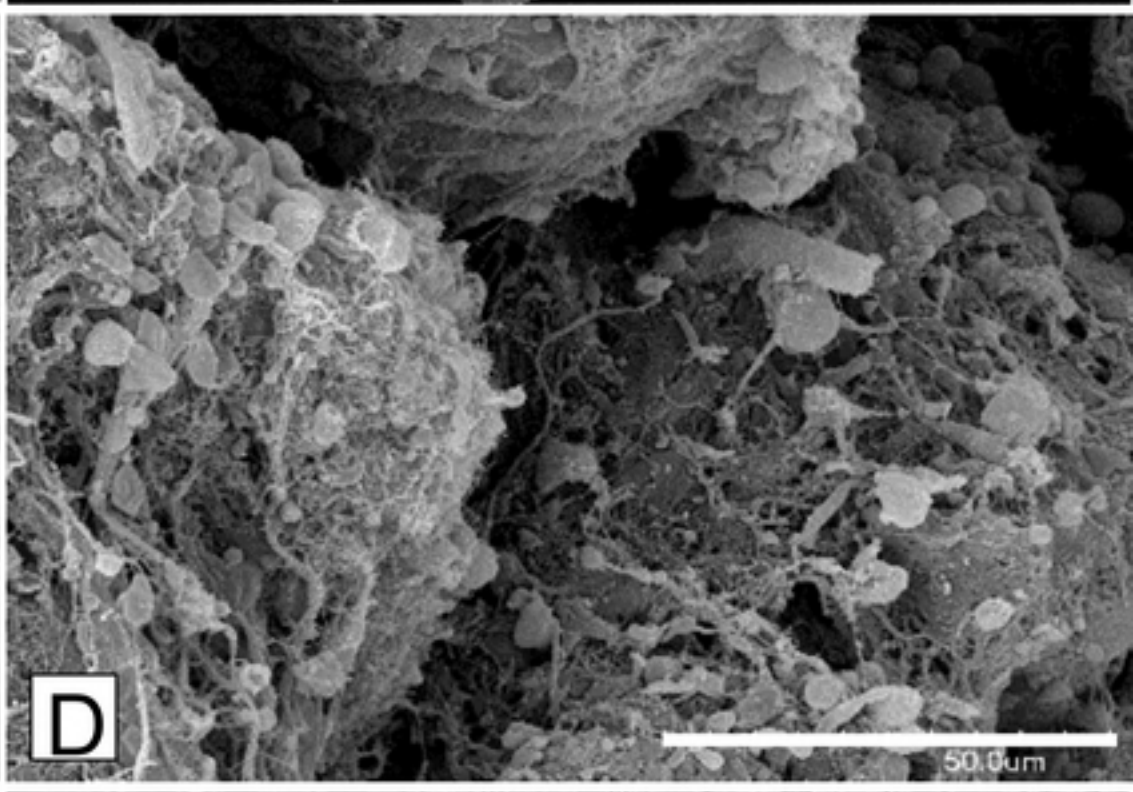

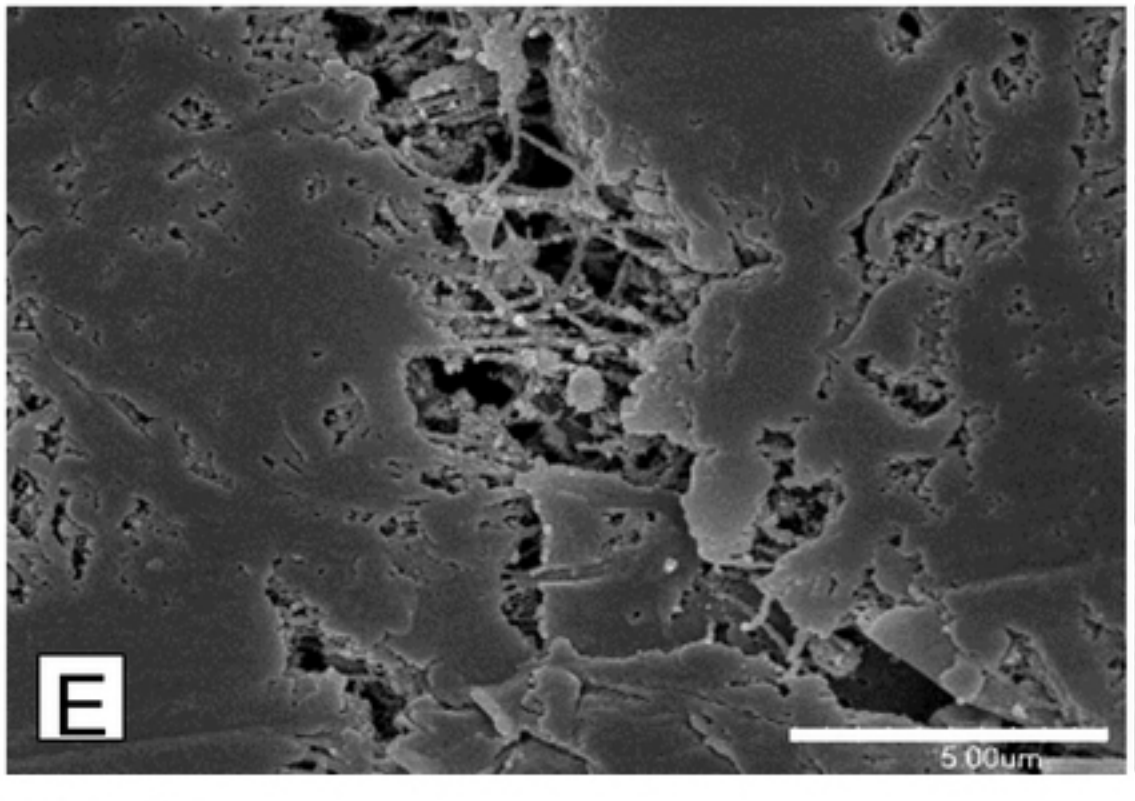

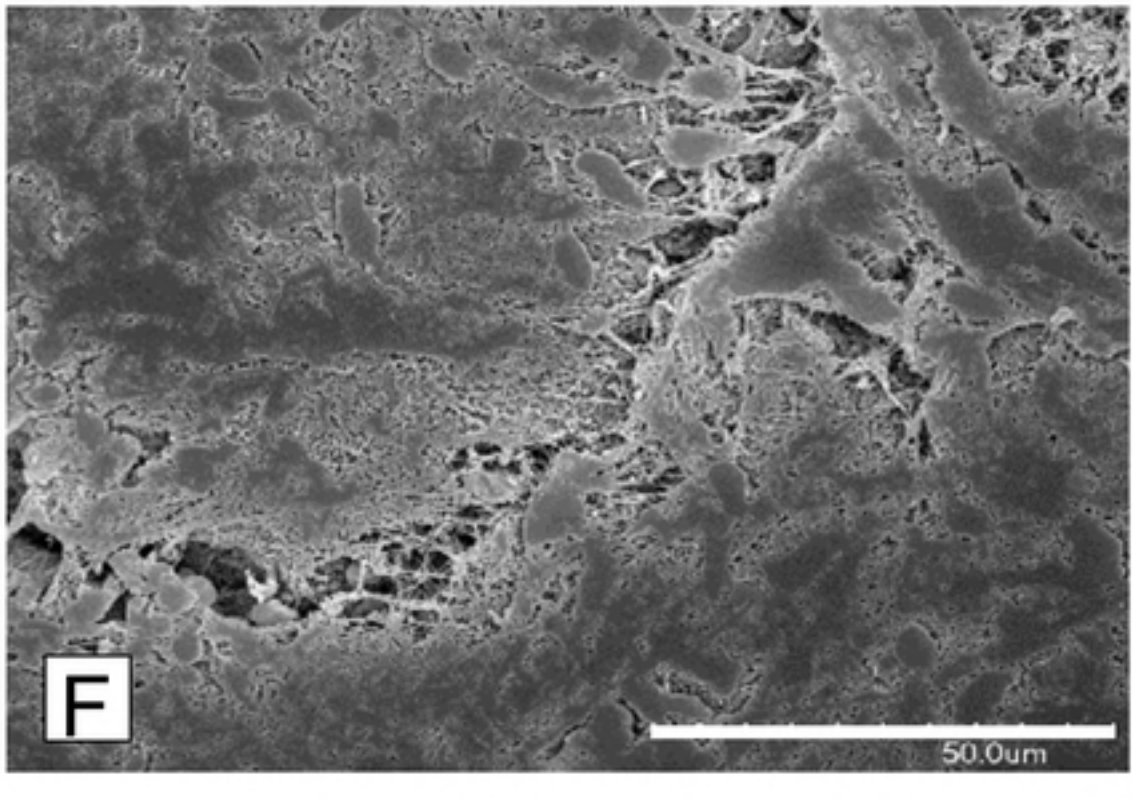

Figure 1a

1b

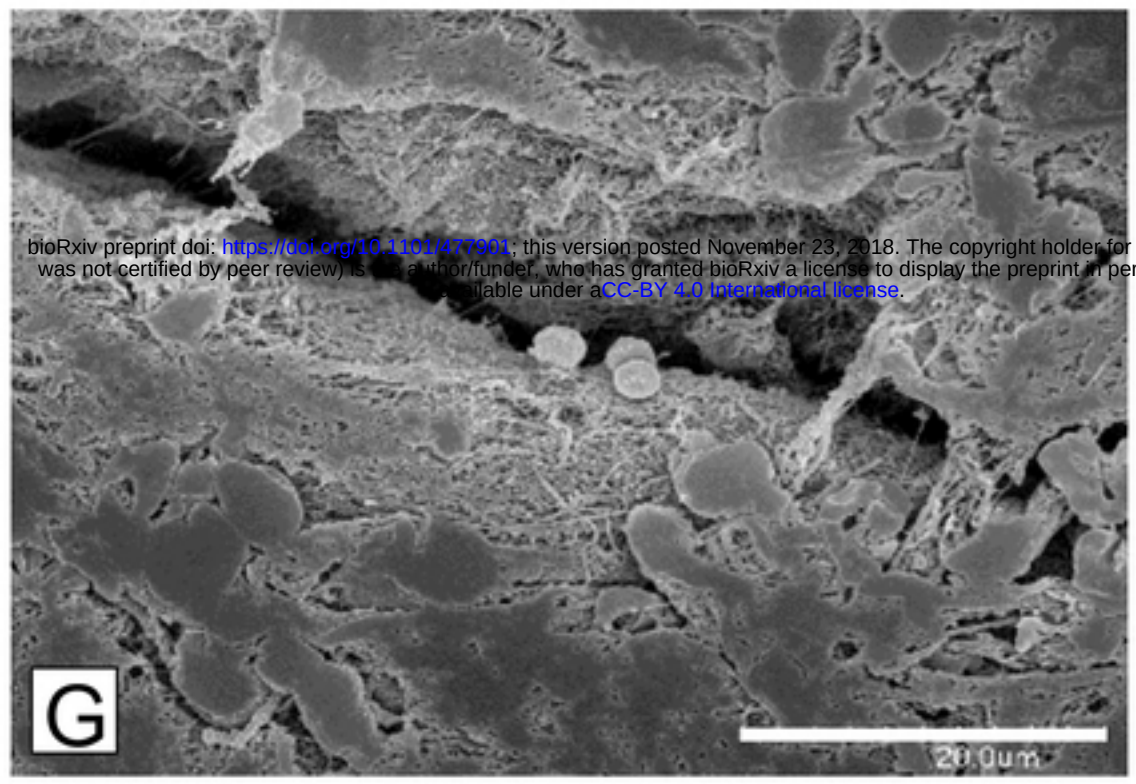

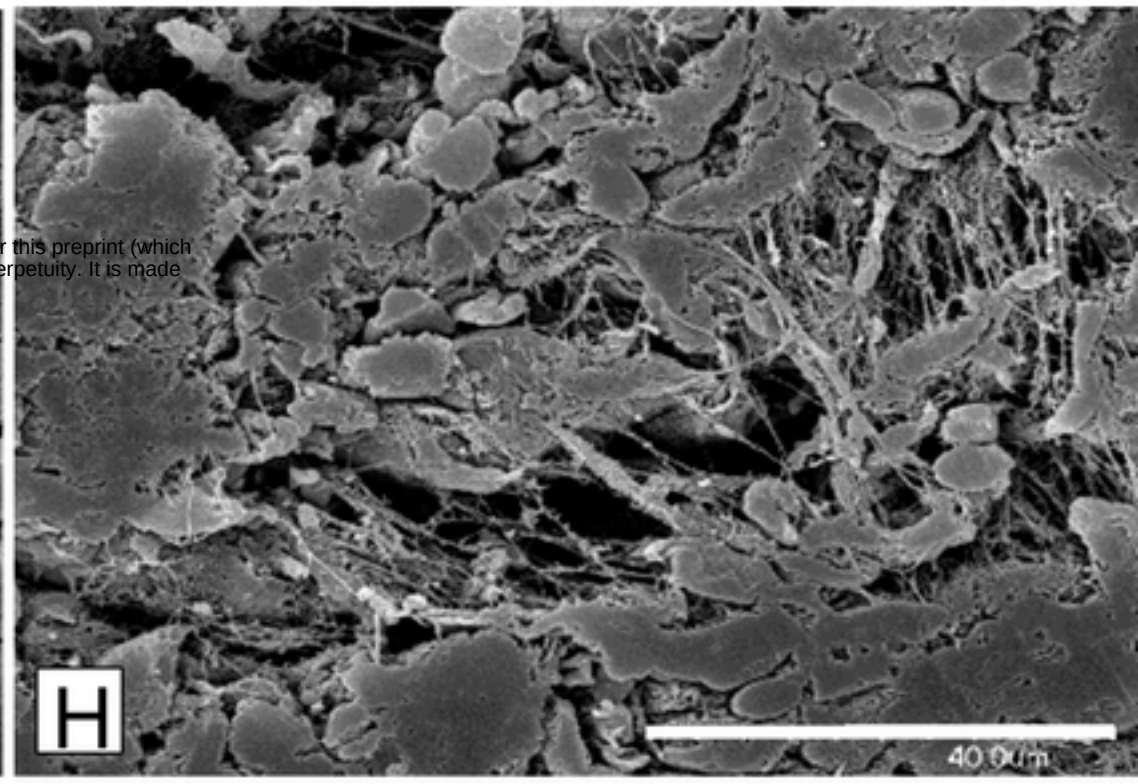

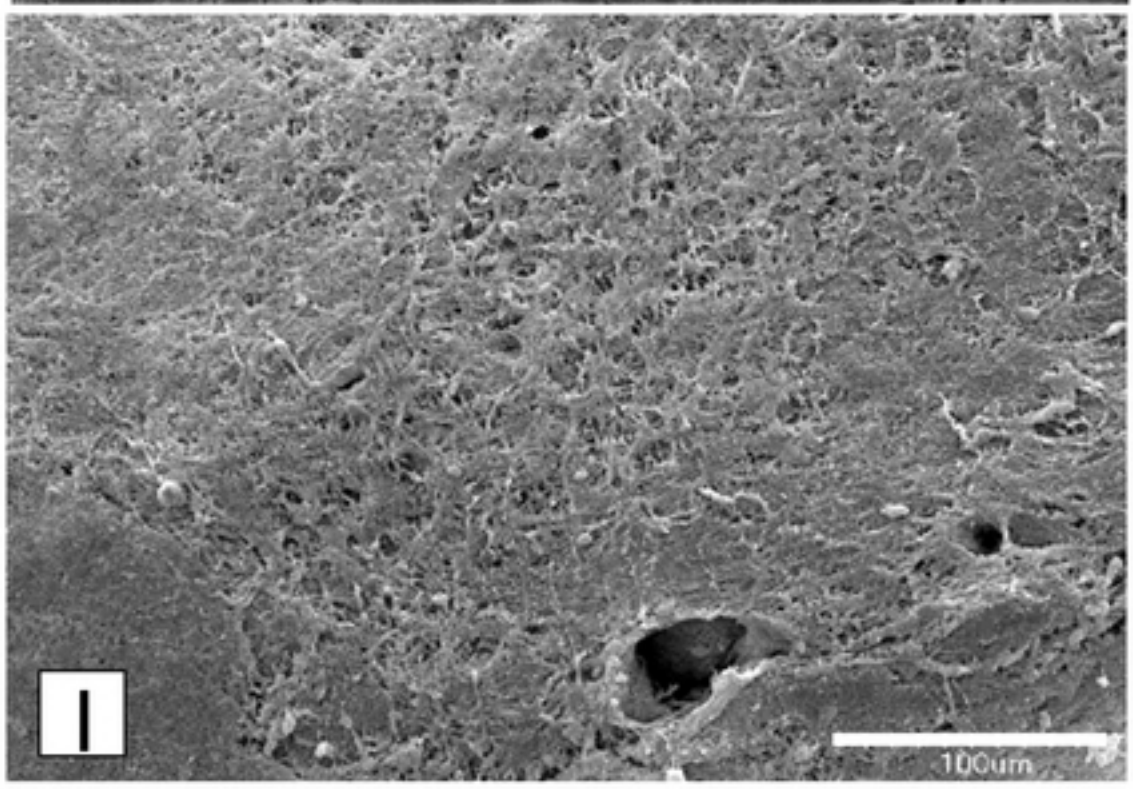

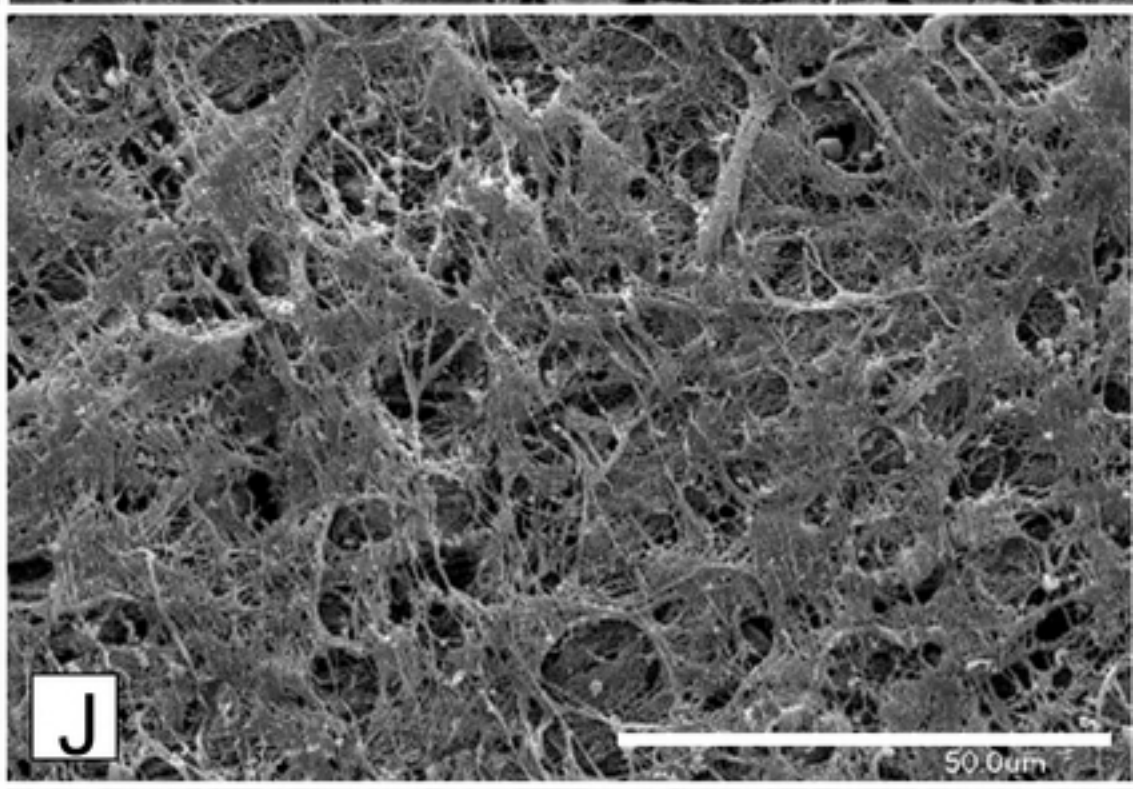

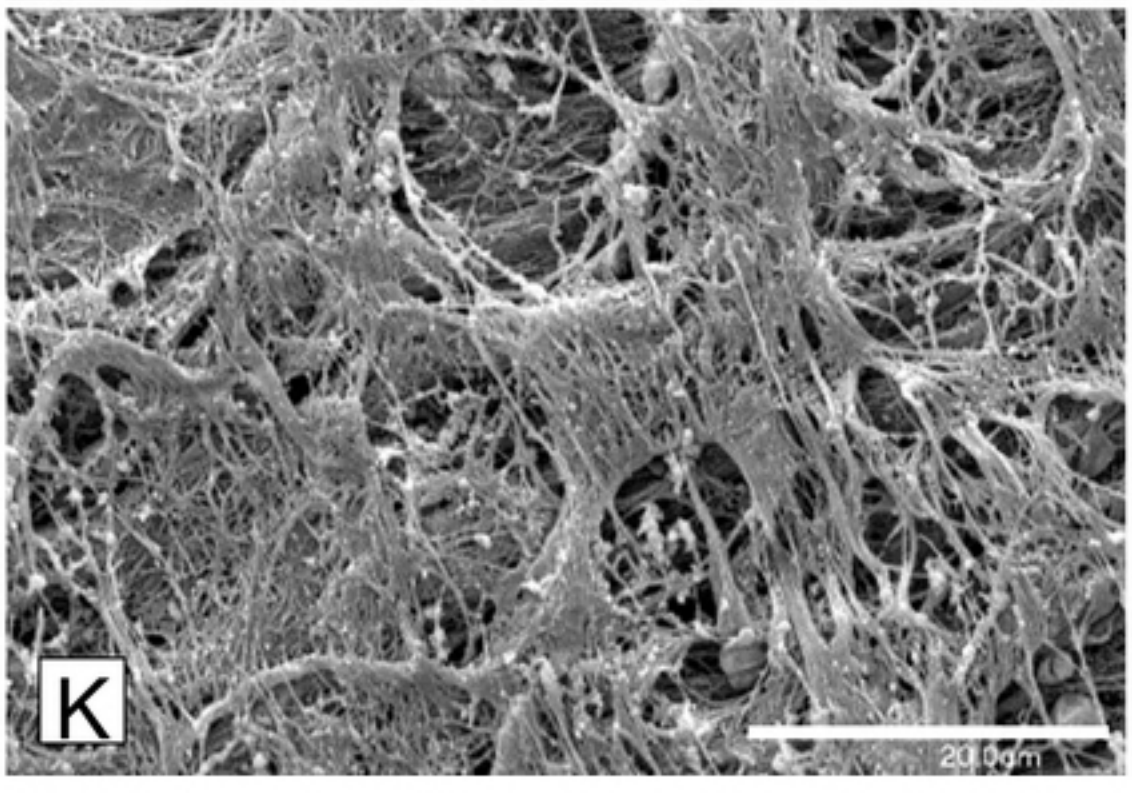

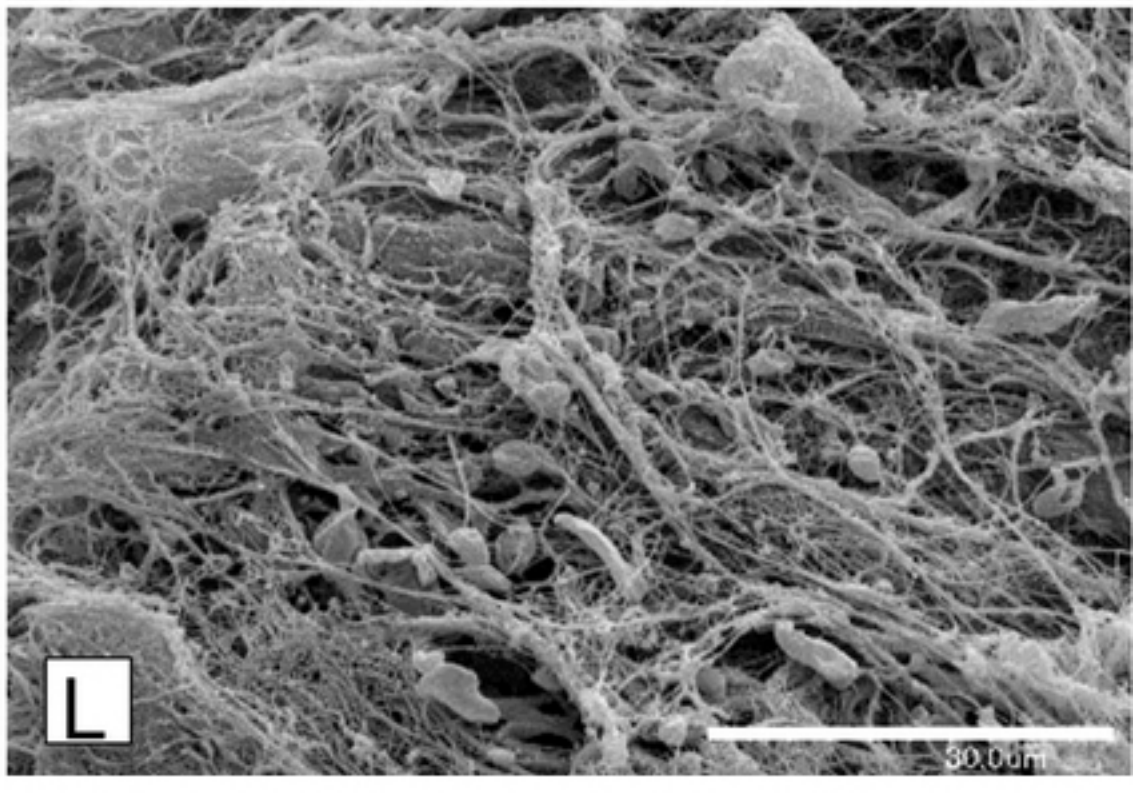

Figure 1b

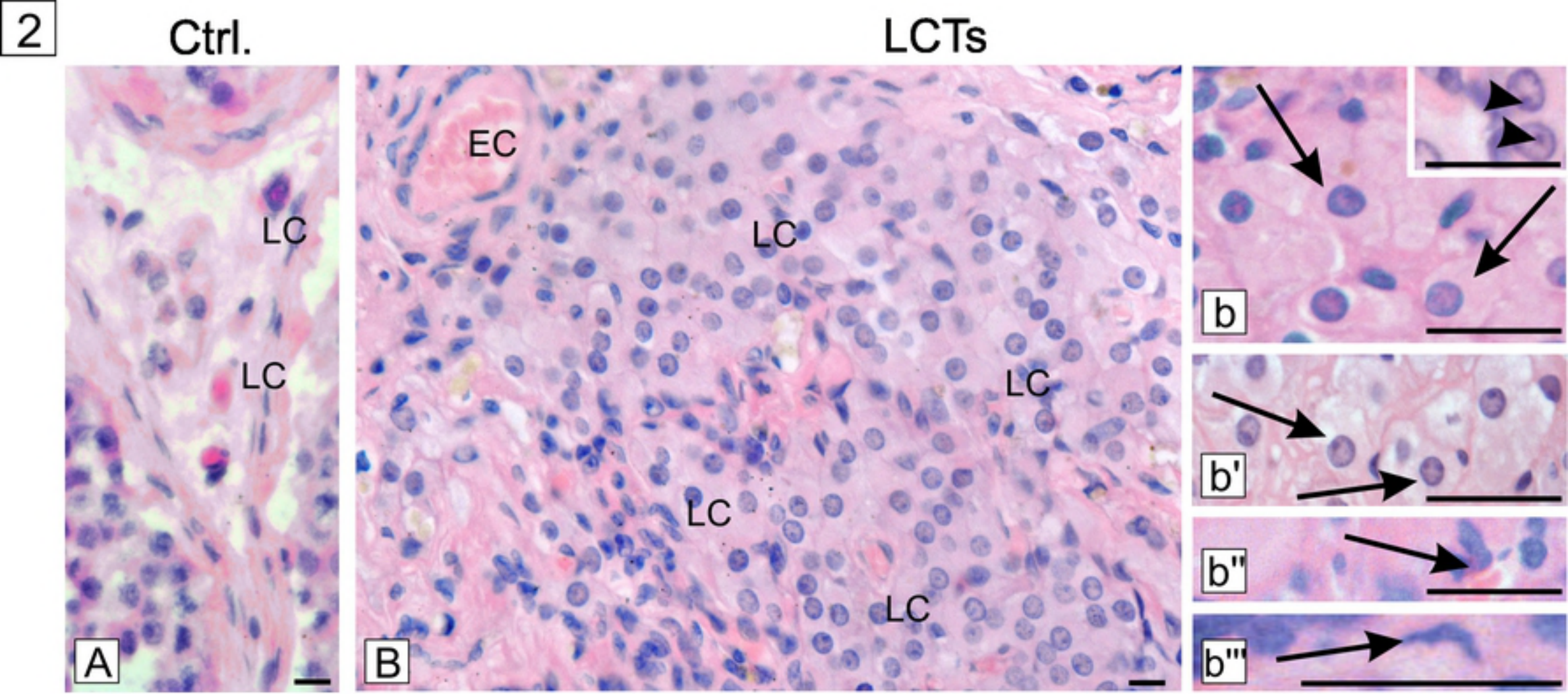

Figure 2

3.

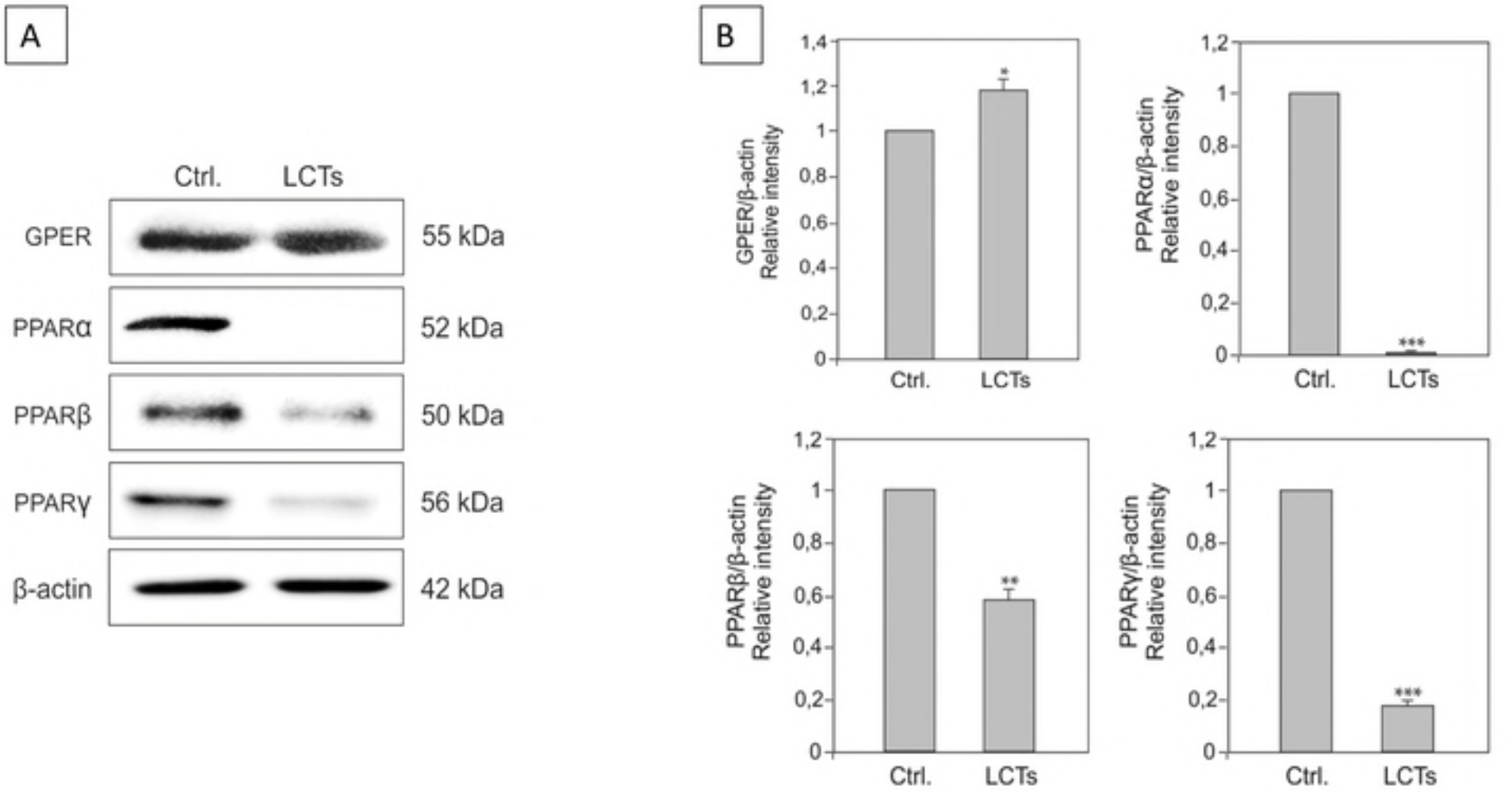
A
Ctrl.
LCTs
GPER
55 kDa
PPARα
52 kDa
PPARβ
50 kDa
PPARγ
56 kDa
β-actin
42 kDa
B
GPER/β-actin Relative intensity
PPARα/β-actin Relative intensity
PPARβ/β-actin Relative intensity
PPARγ/β-actin Relative intensity
Ctrl.
LCTs

Figure 3

4

Ctrl.

LCTs

GPER

A

A'

PPARα

B

B'

PPARβ

C

C'

PPARγ

D

D'

Figure 4

5.

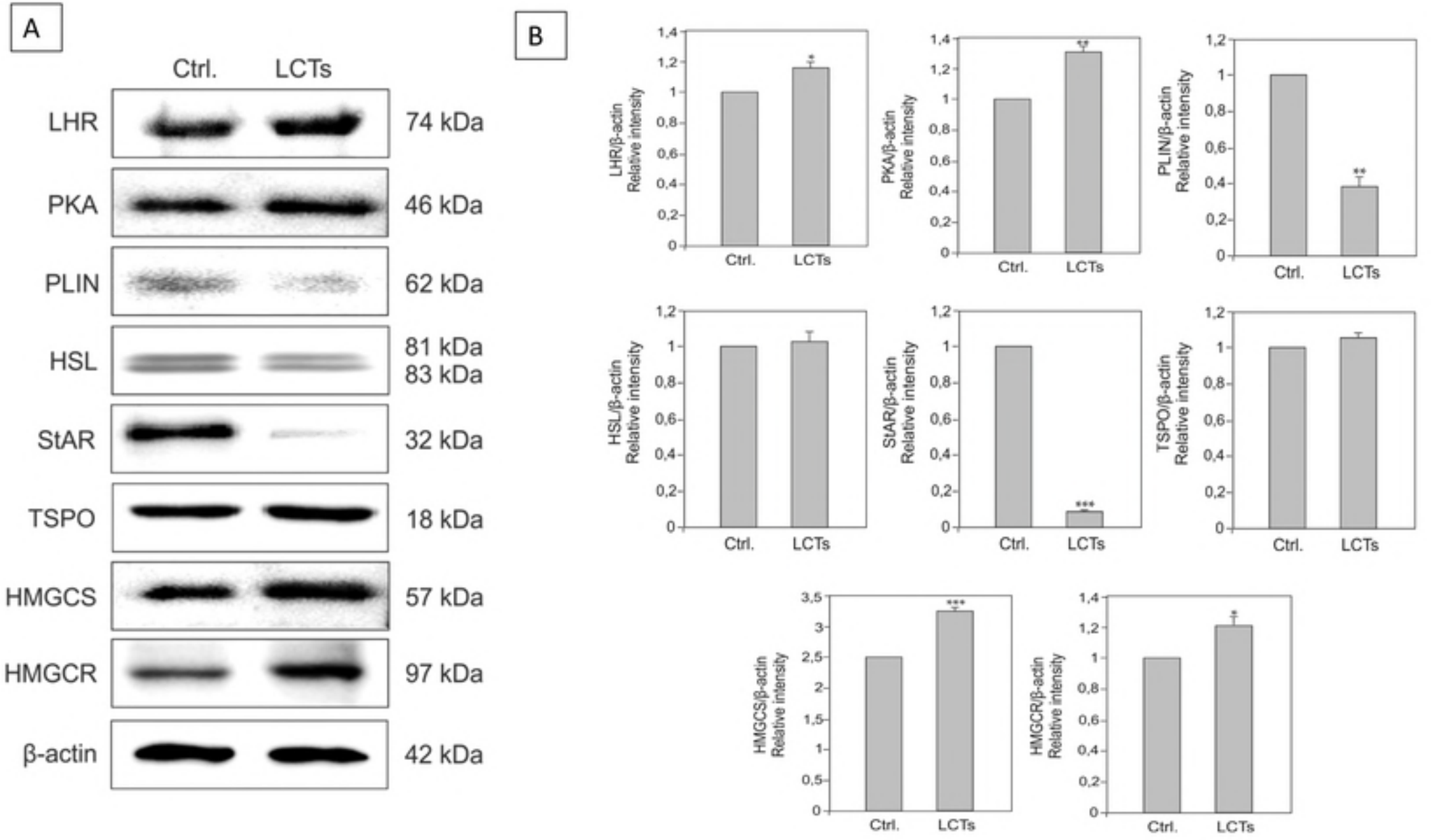
A
Ctrl.
LCTs
LHR
74 kDa
PKA
46 kDa
PLIN
62 kDa
HSL
81 kDa
83 kDa
StAR
32 kDa
TSPO
18 kDa
HMGCS
57 kDa
HMGCR
97 kDa
β-actin
42 kDa
B
LHR/β-actin Relative intensity
PKA/β-actin Relative intensity
PLIN/β-actin Relative intensity
HSL/β-actin Relative intensity
StAR/β-actin Relative intensity
TSPO/β-actin Relative intensity
HMGCS/β-actin Relative intensity
HMGCR/β-actin Relative intensity
Ctrl.
LCTs

Figure 5

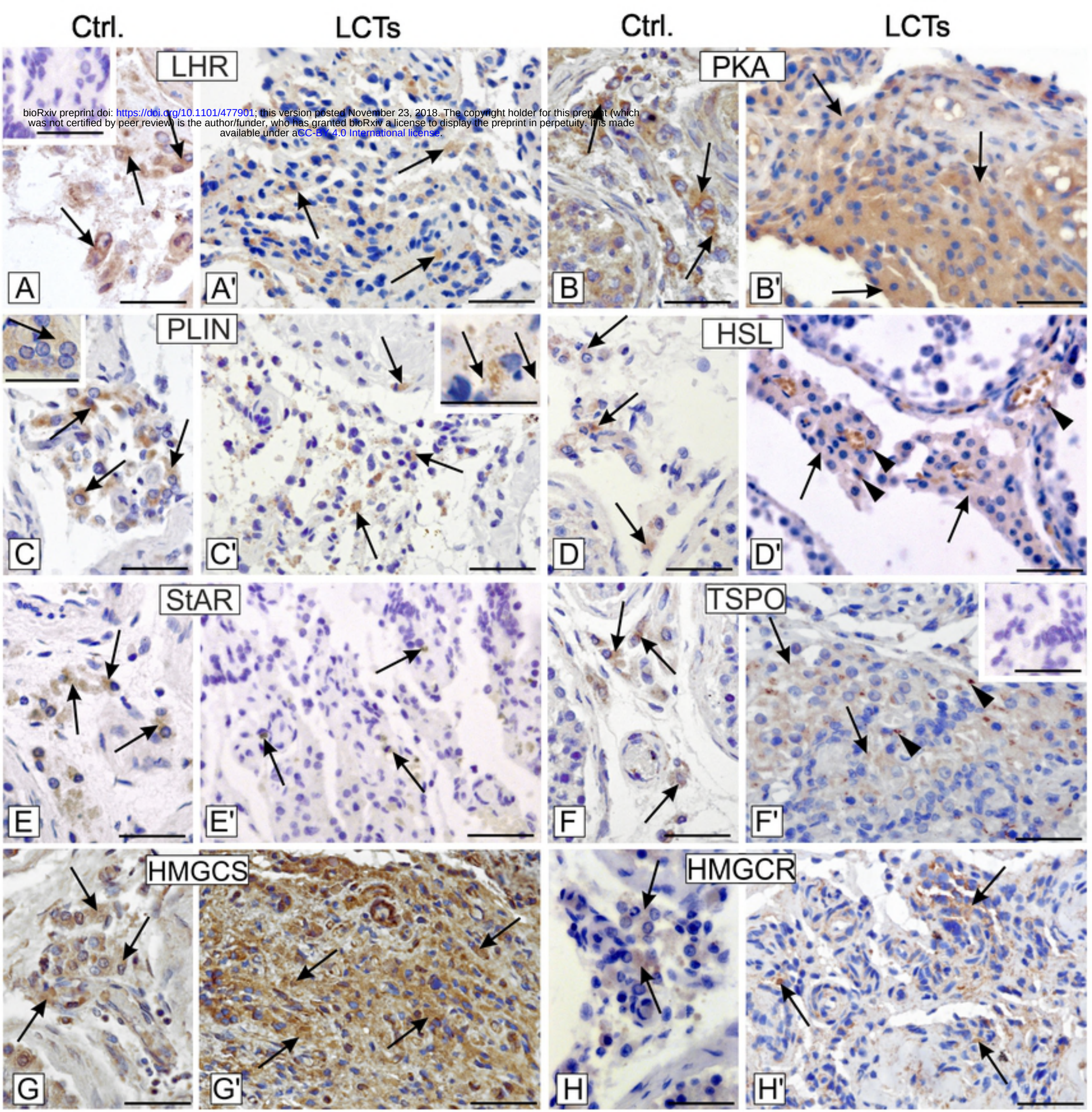

Figure 6

7.

A

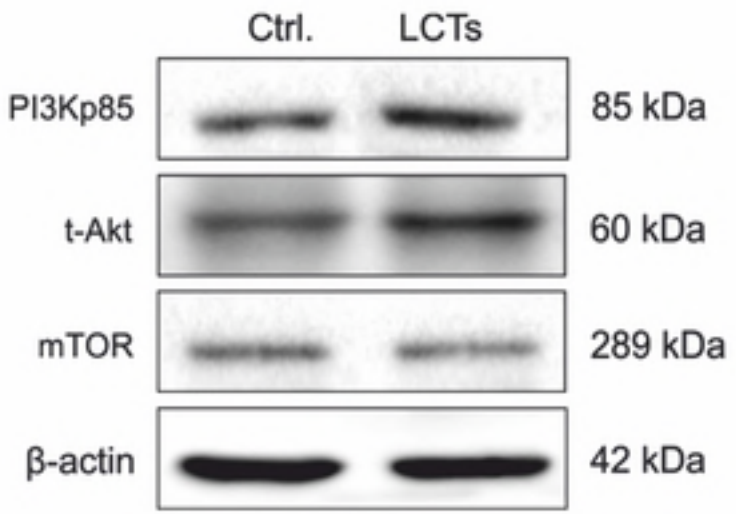
Ctrl.
LCTs
PI3Kp85
85 kDa
t-Akt
60 kDa
mTOR
289 kDa
β-actin
42 kDa

B

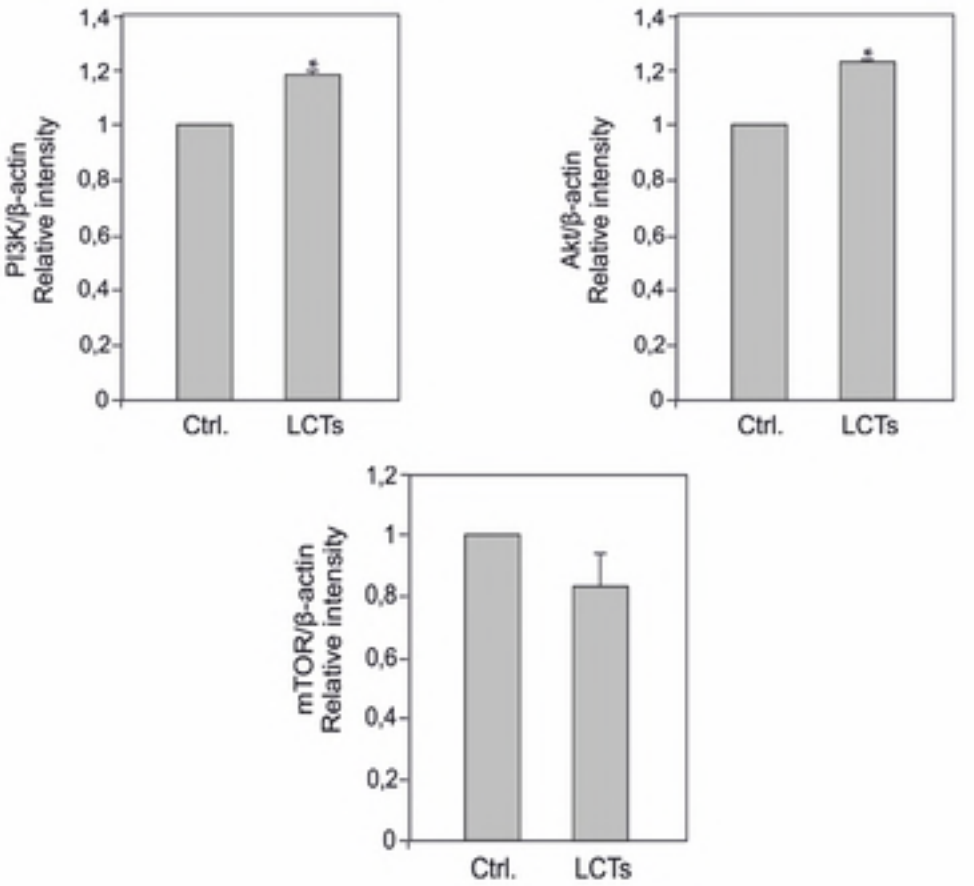
PI3K/β-actin Relative intensity
1,4
1,2
1
0,8
0,6
0,4
0,2
0
Ctrl.
LCTs
*
Akt/β-actin Relative intensity
1,4
1,2
1
0,8
0,6
0,4
0,2
0
Ctrl.
LCTs
*
mTOR/β-actin Relative intensity
1,2
1
0,8
0,6
0,4
0,2
0
Ctrl.
LCTs

Figure 7

8.

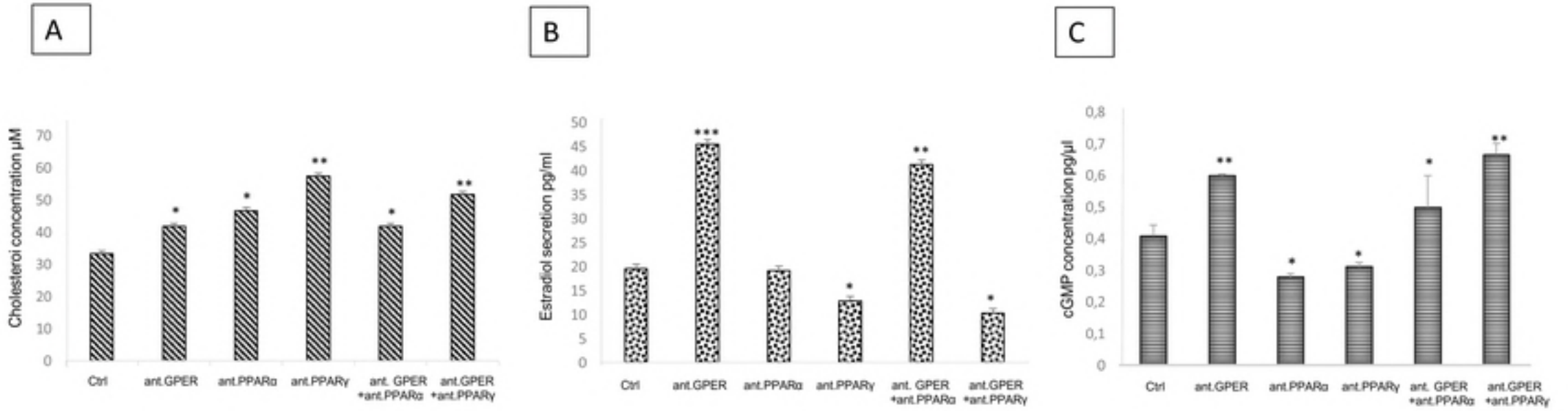
A
Cholesteroi concentration µM
70
60
50
40
30
20
10
0
Ctrl
ant.GPER
ant.PPARα
ant.PPARγ
ant. GPER +ant.PPARα
ant.GPER +ant.PPARγ
B
Estradiol secretion pg/ml
50
45
40
35
30
25
20
15
10
5
0
Ctrl
ant.GPER
ant.PPARα
ant.PPARγ
ant. GPER +ant.PPARα
ant.GPER +ant.PPARγ
C
cGMP concentration pg/µl
0,8
0,7
0,6
0,5
0,4
0,3
0,2
0,1
0
Ctrl
ant.GPER
ant.PPARα
ant.PPARγ
ant. GPER +ant.PPARα
ant.GPER +ant.PPARγ

Figure 8

3’

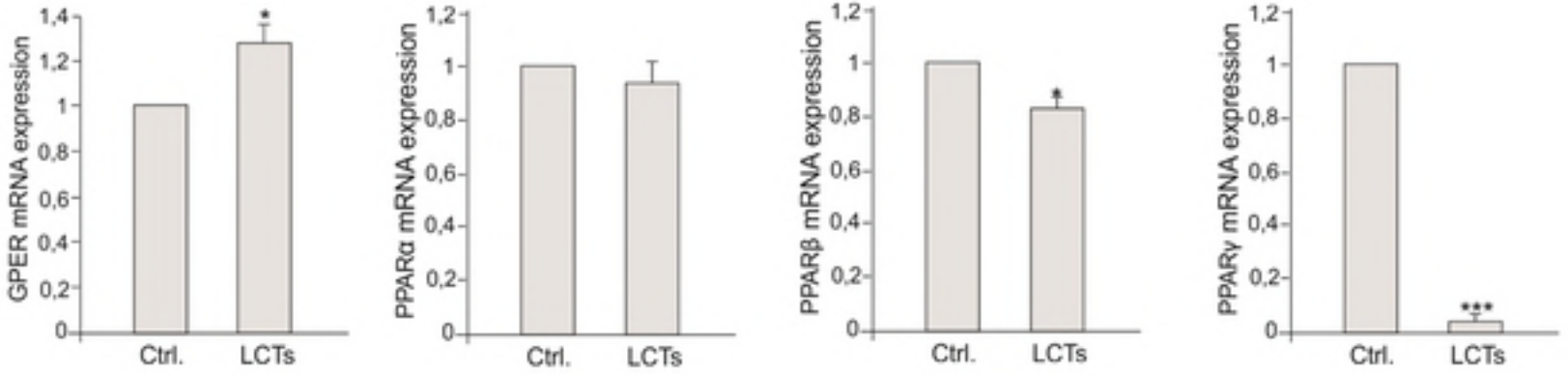

Figure 3prim

5’

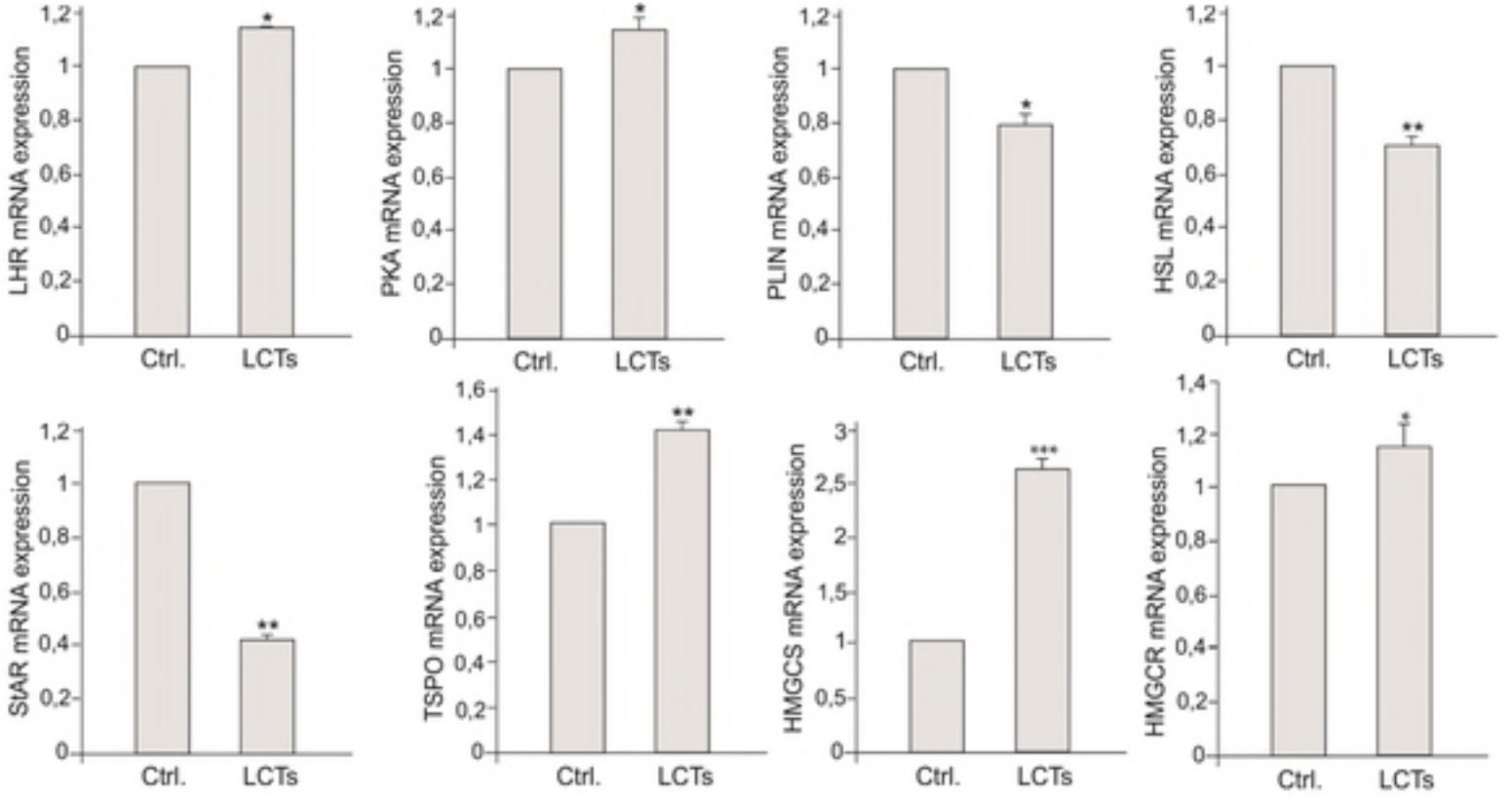

Figure 5prim

7.’ supplementarny

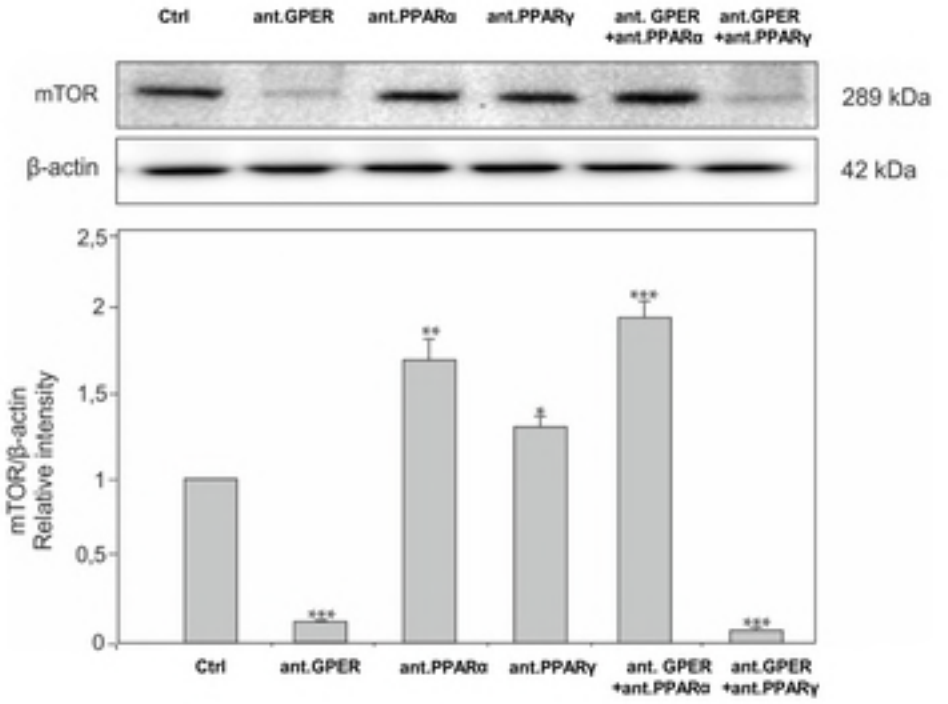

Figure 7prim